

RESEARCH ARTICLE

The use of fluorescence correlation spectroscopy to monitor cell surface β_2 -adrenoceptors at low expression levels in human embryonic stem cell-derived cardiomyocytes and fibroblasts

Joëlle Goulding^{1,2}  | Alexander Kondrashov^{1,3}  | Sarah J. Mistry^{1,4} |
 Tony Melarangi³ | Nguyen T.N. Vo³ | Duc M. Hoang^{3,5} | Carl W. White^{1,2,6,7}  |
 Chris Denning^{1,3}  | Stephen J. Briddon^{1,2}  | Stephen J. Hill^{1,2}

¹Centre of Membrane Proteins and Receptors (COMPARE), University of Nottingham, Nottingham, UK

²Division of Physiology, Pharmacology and Neuroscience, School of Life Sciences, University of Nottingham, Nottingham, UK

³Division of Cancer & Stem Cells, University of Nottingham Biodiscovery Institute, University Park, Nottingham, UK

⁴School of Pharmacy, University of Nottingham, Nottingham, UK

⁵Department of Cellular Manufacturing, Vinmec Research Institute of Stem Cell and Gene Technology, Hanoi, Vietnam

⁶Harry Perkins Institute of Medical Research and Centre for Medical Research, QEII Medical Centre, The University of Western Australia, Nedlands, WA, Australia

⁷Australian Research Council Centre for Personalised Therapeutics Technologies, Melbourne, VIC, Australia

Correspondence

Stephen J. Briddon and Stephen J. Hill,
 Centre of Membrane Proteins and Receptors
 (COMPARE), University of Nottingham,
 Nottingham, UK.

Funding information

RCUK | Medical Research Council (MRC),
 Grant/Award Number: MR/N020081/1;
 British Heart Foundation (BHF), Grant/
 Award Number: RG/14/1/30588;
 Department of Health | National Health
 and Medical Research Council (NHMRC),
 Grant/Award Number: 1088334

Abstract

The importance of cell phenotype in determining the molecular mechanisms underlying β_2 -adrenoceptor (β_2 AR) function has been noted previously when comparing responses in primary cells and recombinant model cell lines. Here, we have generated haplotype-specific SNAP-tagged β_2 AR human embryonic stem (ES) cell lines and applied fluorescence correlation spectroscopy (FCS) to study cell surface receptors in progenitor cells and in differentiated fibroblasts and cardiomyocytes. FCS was able to quantify SNAP-tagged β_2 AR number and diffusion in both ES-derived cardiomyocytes and CRISPR/Cas9 genome-edited HEK293T cells, where the expression level was too low to detect using standard confocal microscopy. These studies demonstrate the power of FCS in investigating cell surface β_2 ARs at the very low expression levels often seen in endogenously expressing cells. Furthermore, the use of ES cell technology in combination with FCS allowed us to demonstrate that cell surface β_2 ARs internalize in response to formoterol-stimulation in ES progenitor cells but not following their differentiation into ES-derived fibroblasts. This indicates that the process of agonist-induced receptor internalization is strongly influenced by cell

Abbreviations: DMEM, Dulbecco's modified Eagle's medium; ES, embryonic stem cell; FBS, fetal bovine serum; FCS, fluorescence correlation spectroscopy; GE, Gly16Glu27; GPCR, G protein-coupled receptor; GRK, G protein-coupled receptor kinase; GQ, Gly16Gln27; HBSS, HEPES-buffered saline solution; OE, over-expression; PCH, photon counting histogram; RE, Arg16Glu27; RQ, Arg16Gln27; SNP, single-nucleotide polymorphism; β_2 AR, β_2 -adrenoceptor.

This is an open access article under the terms of the Creative Commons Attribution License, which permits use, distribution and reproduction in any medium, provided the original work is properly cited.

© 2021 The Authors. *The FASEB Journal* published by Wiley Periodicals LLC on behalf of Federation of American Societies for Experimental Biology.

phenotype and this may have important implications for drug treatment with long-acting β 2AR agonists.

KEYWORDS

cardiomyocytes, differentiation, embryonic stem cells, fibroblasts, fluorescence correlation spectroscopy, haplotype, receptor internalization, single-nucleotide polymorphisms, β 2-adrenoceptors

1 | INTRODUCTION

The β 2-adrenoceptor (β 2AR) is a prototypical member of the class A family of G protein-coupled receptors (GPCRs).¹ Crystal structures of the active β 2AR bound to the partial agonist salmeterol or the native hormone adrenaline, with either a Gs protein or active state-stabilizing nanobodies, have greatly advanced understanding of the pharmacology and activation of β 2ARs.²⁻⁵ Upon ligand stimulation β 2ARs preferentially bind to the heterotrimeric G-protein G α s, stimulating the activation of adenylyl cyclase to catalyze the formation of cyclic AMP from ATP.⁶ Cell surface signaling is terminated following the phosphorylation of the C-terminal domain of the β 2AR by G-protein receptor kinases (GRK), signposting the receptor for beta-arrestin mediated internalization.⁷⁻⁹ This can lead to a second phase of signaling from intracellular endosomes.^{10,11} The β 2AR undergoes ligand-directed internalization via a clathrin-mediated and Rab 5-regulated constitutive endocytic pathway for recycling alongside transferrin, but can also localize to lysosomes if directed toward a degradation pathway.¹²⁻¹⁶

The β 2AR has been shown to display distinct trafficking profiles dependent on the presence of single-nucleotide polymorphisms (SNPs).¹⁷⁻²⁰ While there are a number of SNPs present in the human β 2AR only four result in altered amino acids; Arg16Gly, Glu27Gln, Val34Met, and Thr164Ile.²¹⁻²³ Within the human population, Arg16Gly and Glu27Gln are most common and these are present in the N-terminus region.^{18,19} The relative frequency of these genotypes within the human population varies with race²⁴; however, linkage disequilibrium leads to the Arg16Glu27 haplotype being extremely rare.²⁵

Cell phenotype has been shown to be important in determining the nature of the molecular mechanisms underlying β 2AR function and regulation.^{7,14,26} For instance, responses to β AR agonists differ dramatically between primary vascular smooth muscle cells and recombinant HEK293 systems.²⁶ Similarly, clustering of β 2ARs has been demonstrated in cardiomyocyte-like rat H29C cells but not in HeLa or CHO cell lines.¹⁴ Cell type specificity is likely to be dictated by the expression levels of both the β 2AR and its effector proteins, as observed in the case of the GRK subtype responsible for β 2AR phosphorylation.⁷ To determine these molecular

mechanisms, single-molecule imaging techniques have been employed which have the sensitivity necessary to expose the spatial and temporal characteristics of these short-lived effects.²⁷⁻³¹ Coupling of single-molecule imaging techniques with the use of human embryonic stem (ES) cells, that can be induced to differentiate into multiple cell phenotypes, provides a potential approach to study the impact of cell phenotype on receptor pharmacology.³²⁻³⁴

An important consideration is the need to work at low receptor expression levels similar to those seen endogenously to limit the impact of receptor over-expression.^{35,36} A drawback of imaging endogenous GPCRs using standard light microscopy within their native environment; however, is that low levels of endogenous receptor expression can lead to poor signal to noise ratios.^{37,38} One approach with the sensitivity to monitor receptors in membrane microdomains at very low receptor expression levels is fluorescence correlation spectroscopy (FCS).³⁹⁻⁴⁴ Here, we have generated haplotype-specific SNAP-tagged β 2AR human ES cell lines and applied FCS to monitor cell surface receptors in differentiated fibroblasts and cardiomyocytes.

2 | METHODS

2.1 | Creation of SNAP β 2AR construct

To create the pSIN-B2-BSD(RQ) lentiviral construct we PCR amplified the Arg16Gln27 (RQ) variant of SNAP β 2AR from the pcDNA3.1(Neo+)sig.SNAP(Met > Leu mutant) expression vector⁴⁵ with the following primer pairs: Fwd1-CTTAAaCTaGtTACCGCCACCATGCGGCTCTGC and Rev1-TCTGCAGAATTCTTACAGCAGTGAGTCATTTG, and after digestion with SpeI and EcoRI restriction enzymes cloned it into the SpeI/EcoRI pSIN-BSD lentiviral vector backbone produced from the pSIN-GFP-BSD plasmid.⁴⁶ All remaining haplotypes variants were created by a PCR-splice mutagenesis technique⁴⁷ using the pSIN-B2-BSD(RQ) construct as a template, with the following set of overlapping primers: G79C Fwd 5'-CGTACAGCAGGAAAGGGACGAG-3' & G79C Rev 5'-CTCGTCCCTTTCCTGCGTGACG for changing position 79 of β 2AR; and G48A Fwd 5'-CTGGCACCCAATGGAAGCCATG & G48A Rev

5'-ATGGCTTCCATTGGGTGCCAG, for substituting A for G at position 48 of β 2AR. The following two primers were used as flanking primers for all PCR-splice reactions: Fwd2-CATTCTCAAGCCTCAGACAGTGG and Rev2 5'-AAATCACATATAGACAAACGCACAC. The final PCR products for each corrected SNP variant were SpeI/EcoRI digested and cloned into the pSIN-BSD SpeI/EcoRI backbone as described above. In total three vectors were produced from pSIN-B2-BSD(RQ) which were: pSIN-B2-BSD(RE), pSIN-B2-BSD(GQ), and pSIN-B2-BSD(GE) which represent the four different haplotypes involving the single-nuclear polymorphisms at Arg16Gly and Glu27Gln. In order to generate lentiviral particles, each construct was transfected together with packaging vectors in to a BL15 cell line and the particles produced were purified on streptavidin paramagnetic beads (Promega) as described in detail earlier.^{48,49} Purified viral particles were used to transduce HEK293T and HUES7 cell lines at MOI of 10. Twenty-four hours following transduction, growth media was exchanged for fresh medium and after 48 hours Blasticidin (Thermo Fisher Scientific) was added to the media at a concentration of 2.5 μ g/mL for HEK293T and 2 μ g/mL for HUES7 cells. A population of antibiotic-resistant cells was expanded in culture for 3 weeks before being banked for further experimental use.

2.2 | CRISPR/Cas9 genome-engineering of HEK293T cells

Generation of constructs for CRISPR/Cas9 genome-engineering of the N-terminal region of the β 2AR genomic locus was performed as described previously¹⁶ with the following modification: Following synthesis of the β 2AR donor repair template, sig-SNAP⁴⁵ was ligated into the repair template using the restriction enzymes KpnI and BamHI. A mutation introduced during the synthesis of the donor repair template to eliminate an internal KpnI restriction site was then corrected by site-directed mutagenesis using primers described previously.¹⁶ The donor template, therefore, resulted in cells expressing genome-edited sig-SNAP β 2AR with the start codon (Met) of the β 2AR deleted.

CRISPR/Cas9 genome-engineering of the β 2AR genomic locus in HEK293T was performed as described previously.⁵⁰ Briefly, HEK293T cells were seeded into six well plates and incubated for 24 hours at 37°C/5% CO₂. HEK293T cells were cultured in DMEM supplemented with 10% fetal bovine serum (FBS). At 60% confluency, cells were transfected with px459 sgRNA/Cas9 expression constructs¹⁶ and the donor repair template encoding sig-SNAP β 2AR using FuGENE transfection reagent (Promega). Twenty-four hours later cells were cultured with puromycin (0.3 μ g/mL, Sigma-Aldrich) for 3 days. Following selection, cells were cultured

without puromycin and seeded into clear flat bottom 96-well plates at 1 cell per well and allowed to expand for 2-3 weeks. Single colonies were then seeded into duplicate 48 well plates and allowed to expand. To screen for positive clones, genomic DNA was extracted using a Wizard Genomic DNA Purification Kit (Promega) and PCR performed using the following primers 5'-CGAGTGTGCTGAGGAAATCA-3' and 5'-CGCCAGAGCTAGACACCAC-3'. The primers used were designed to anneal outside the left homology arm of the donor repair template and the SNAP tag, respectively. Positive clones were expanded prior to use.

2.3 | Cell culture

Transgenic and non-transgenic HEK293T cells were maintained in growth media at 37°C 5% CO₂; Dulbecco modified eagles medium (DMEM) supplemented with 10% fetal bovine serum (FBS). In the case of transgenic lines, the growth medium also contained blasticidin (2.5 μ g/mL). Once confluent, cells were dislodged from the flask surface by gentle shaking after incubation in 0.25% trypsin and a cell pellet formed following 5 minutes 1000 g centrifugation. For subsequent assays, cells were re-suspended in DMEM supplemented with 10% FBS and seeded at a density of 40-50 000 cells/well on poly-D-lysine treated clear-bottomed white-walled (radioligand binding), black-walled (internalization assay) 96 well plates or 8-well Nunc Lab-tek chambered coverglass (No. 1.0 borosilicate glass bottom) (imaging). Cells were incubated at 37°C 5% CO₂ overnight prior to assay.

The human embryonic stem cell line, HUES7 (ES), was gifted from Harvard University under Material Transfer Agreement⁵¹ and approved for use by the UK Stem Cell Steering Committee (Ref no 17/12/2007). Undifferentiated cells were cultured under feeder-free conditions on Matrigel-coated surfaces in the presence of MEF (mouse embryonic fibroblast) conditioned medium supplemented with 4 ng/mL of bFGF (basic fibroblast growth factor), as previously described.^{34,49} Transgenic haplotype variant lines were maintained in the same conditions in presence of 2 μ g/mL of blasticidin in order to maintain the expression level of transgenes. For monolayer differentiation into cardiomyocytes, cells were first transitioned to the E8 culture medium (Life Technologies) and banked, and then differentiated as previously described.⁵² Fibroblast differentiation was as follows: Transgenic cell lines were first seeded at 40 000 cells/cm² in a Matrigel-coated T25 flask and cultured in Essential 8 medium until reaching 80% confluence. The culture was then treated with StemPro34 (Life Technologies) medium supplemented with 10 ng/mL of BMP4 (bone morphogenetic protein 4, R&D systems) and 8 ng/mL of Activin A (Life Technologies) and cultured for 48 hours; on day 2, the medium was switched into RPMI medium added with

B27 supplement and 10% FBS; on day 4, the medium was changed into the fibroblast culture medium, which containing DMEM supplemented with 10% FBS, 1X GlutaMAX and 1X NEAA (non-essential amino acids). Differentiation into specific cell types was confirmed by immunohistochemistry to identify cell type-specific markers (Supporting Information Figure S1).

2.4 | Radioligand binding

Cells were plated at densities of 50 000 (HEK293T) or 70 000 (ES) cells per well in white-walled, clear-bottomed 96 well plates in growth media and left overnight. Growth media was aspirated and cells were incubated in 100 μ L serum-free media (HEK293T:DMEM; ES: RPMI conditioned media supplemented with B27 supplement (Life Technologies)) in the presence or absence of 10 pM–10 μ M of CGP 12177, CGP 20712A, ICI 118551 or propranolol (for competition binding assays), and the presence or absence of 10 μ M propranolol (for saturation binding assays). The addition of 100 μ L of serum-free medium or serum-free medium containing 0.01–20 nM (saturation) 3 H-CGP 12177 immediately followed and cells were incubated for 2 hours at 37°C 5% CO₂. Cells were washed twice in PBS (Phosphate Buffered Saline) and 200 μ L Microscint 20 added to each well and a white bottom and a topseal added to each plate. Plates were then left overnight and readings taken (counts per minute; CPM) on a TopCount Microplate Scintillation Counter (Packard Instrument, CT).

2.5 | SNAP labeling

The SNAP-tag labeling system allows real-time live-cell imaging of the protein of interest following labeling of the 20 kDa SNAP-tag which can be engineered to be expressed on the N- or C- terminus of the protein. The SNAP-tag represents O⁶-alkylguanine-DNA alkyltransferase that reacts specifically and rapidly with benzylguanine (BG) derivatives resulting in an irreversible covalent linking with a fluorescent probe.⁵³ Cells were incubated in growth medium in the presence of 0.5 μ M (imaging), 0.1–2 μ M (internalization assay) or 0.1 μ M (fluorescence correlation spectroscopy; FCS) SNAP-Surface Alexa Fluor 488 (SNAP-488) for 30 minutes at 37°C. Following this, cells were then washed twice in warmed appropriate imaging buffer. HBSS (HEPES-buffered saline solution pH 7.45; Sodium pyruvate 2 mM, NaCl 145 mM, D-Glucose 10 mM, KCl 5 mM, MgSO₄·7H₂O 1 mM, HEPES 10 mM, CaCl₂ 1.7 mM, NaHCO₃ 1.5 mM) was used for HEK293T cells. ES-HBSS (HEPES-buffered saline solution pH 7.45; NaCl 140 mM, D-Glucose 10 mM, KCl 4 mM, MgCl₂ 1 mM, HEPES 10 mM) was used for

ES progenitor cells, ES-derived fibroblasts, and ES-derived cardiomyocytes.

2.6 | Confocal microscopy

Cells were plated at varying densities on 8-well Nunc Labtek chambered coverglasses in growth media and left overnight. Slides were pre-coated with poly-D-lysine (HEK293T) or Matrigel (ES progenitor cells and cardiomyocytes) or used without pre-coating in the case of fibroblasts. The following day the media was removed and cells were SNAP labeled with SNAP-Surface Alexa Fluor 488 (SNAP-488) as described above. Cells were imaged on either the Zeiss LSM710 or Zeiss LSM880 confocal microscopes, both with a Zeiss Axio Observer Z1 stand (Carl Zeiss, Germany) using 488 nm Argon laser excitation (to image SNAP-488), a 493–630 nm emission range, and a plan-apochromat 40 \times 1.2NA oil immersion objective. Pinhole was set at 1 airy unit and gain and offset settings were kept constant within the experimental day. Cells were imaged in the presence or absence of formoterol and processed using Zen Black (2012) software (Carl Zeiss, Germany).

2.7 | Immunocytochemistry

To confirm the cell type of ES-derived fibroblasts and ES-derived cardiomyocytes, the dissociated fibroblasts and cardiomyocytes were seeded into Matrigel-coated 96-well plate at 55,000 cells/well and maintained for at least 3 days. The culture was fixed with 4% paraformaldehyde (diluted in PBS) for 12 minutes prior to being stored at 4°C for up to one week. On an experimental day, cells were incubated with 0.01% Triton X-100 (diluted in PBS) for 15 minutes and washed twice in 0.05% Tween 20 (diluted in PBS) to perforate membranes. Cells were then incubated in 5% human serum (diluted in PBS) for 30 minutes prior to antibody treatments. The fibroblast cultures were incubated for 1 hour with primary sheep anti-human CD90 antibody (No. AF2067, 1:50 dilution, R&D systems) and then 1 hour with secondary donkey anti-sheep AlexaFluor633 (No. A21448, 1:500 dilution, Thermo Fisher Scientific). The cardiomyocytes were incubated for 1 hour with primary mouse anti-human α -actinin antibody (No. A7811, 1:800 dilution, Sigma-Aldrich) and 1 hour with secondary goat anti-mouse AlexaFluor 488 (No. A11001, 1:1000 dilution, Thermo Fisher Scientific). Both cell types were incubated for 15 minutes with 0.5 μ g/mL of DAPI (No. D9542, 1:500 dilution, Sigma-Aldrich) to stain nuclear regions. Immunofluorescence images were captured with a 20 \times NA 0.45 long working distance objective on an Operetta High-Content System (PerkinElmer, UK) with a 300 W Xenon lamp (360–640 nm continuous spectrum) laser excitation.

Excitation filter and emission bandpass filters were for DAPI 380/40 and 445/70, AlexaFluor488 475/30 and 525/50 and for AlexaFluor633 630/20 and 705/110. Images were analyzed using Harmony High-Content Analysis software.

2.8 | Ligand-induced receptor internalization

Cells were plated at densities of 40 000 (HEK293T) or 70 000 (ES progenitor) cells per well in poly-D-lysine/Matrigel-coated black-walled, clear-bottomed 96 well Greiner plates in growth media and left overnight. The following day, the media was removed and cells were labeled with SNAP-488 as described above. Following labeling the cells were washed once in imaging buffer (HBSS or modified ES:HBSS), and then incubated for 1h in imaging buffer in the presence or absence of 100 μ L formoterol (10 pM-1 μ M), salbutamol (100 pM-100 μ M) or salmeterol (1 pM-10 μ M). Buffer was then removed and cells washed once more in buffer and then fixed by incubating in 10% ice-cold formalin solution (in PBS) for 15 minutes prior to 10 minutes incubation in ice-cold PBS and a 15 minutes incubation in PBS containing 2 μ g/mL of Hoechst 33342 stain. Cells were then washed once in PBS and then 100 μ L PBS replaced per well and the 96-well plate was wrapped in foil and stored at 4°C for at least 24h. Four confocal images were recorded per well on the Molecular Devices ImageXpress Ultra confocal plate reader (Molecular Devices, CA) equipped with a Plan Fluor 40x NA 0.6 extra-long working distance objective using 405 nm laser excitation with a 477/60 band pass filter (to image Hoechst 33342) and 488 nm laser excitation with a 525/50 band pass filter (to image SNAP-488). The images were analyzed using the granularity analysis algorithm within the MetaXpress software (Molecular Devices, CA) which identifies fluorescent species, “granules,” defined by a fluorescence intensity threshold and size limits. Size limits detailing SNAP-labeled receptor or Hoechst 33342 stained nuclear regions, for both cell types are as follows. HEK293T; receptor 7-15 μ m in width and nuclear regions 6-9 μ m in width. ES; receptor 1-3 μ m in width and nuclear regions 5-15 μ m in width. As the intensity of these regions depended on the efficiency of their labeling, threshold background levels were set per plate and data were normalized to allow comparison across experiments.

2.9 | Fluorescence correlation spectroscopy

Cells were plated on 8-well Nunc Lab-tek chambered coverglass (No. 1.0 borosilicate glass bottom) pre-coated with Matrigel (ES progenitor cells, cardiomyocytes),

poly-D-lysine (HEK293T) or without coating (fibroblasts) in growth media and left at least 24h before analysis. Cells were labeled with SNAP-488 (0.1 μ M) for 30 minutes at 37°C and then washed twice in warm imaging buffer followed by a longer 20 minutes wash before finally being left in 180 μ L imaging buffer at 37°C until use. Cells were then incubated in the absence or presence of the β 2AR agonist, formoterol (10 minutes, 10 nM, 37°C) before being allowed to cool to 24°C. FCS readings were taken on either a Zeiss LSM880 microscope on a Zeiss Axio Observer Z1 stand (HEK293T) or on a Zeiss LSM510NLO ConfoCor 3 microscope (ES progenitor cells, fibroblasts, cardiomyocytes) both fitted with 40X c-Apochromat 1.2 NA water-immersion objectives using an Argon laser at 488 nm excitation with emission collected through a 505-610BP filter (LSM10NLO) or a 508-691 BP (LSM880) and the pinhole set to 1 Airy unit as previously described.⁵⁴ Briefly, the detection volume was positioned in x-y using a live confocal image and then in z following an intensity z-scan ± 2 μ m (in 0.25 μ m intervals) from the approximated membrane position. For HEK293T cells, the detection volume was placed at the peak of the intensity z-scan and fluorescent fluctuations collected for 1 \times 20-30s at ~ 0.5 kW/cm² laser power. For ES and progenitor cells sequential 1 \times 20-30s reads at ~ 0.5 kW/cm² laser power were taken at successively decreasing z positions (0.25-0.50 μ m intervals) on the same cell and the membrane trace was identified from the first trace to show typical membrane fluctuation patterns and the associated autocorrelation curves.

Autocorrelation curves were analyzed within Zen Black (2012) software and fitted with a diffusion model consisting of two components, the first depicting a 3D (free SNAP) and the second a 2D (receptor) diffusing component.⁴² The autocorrelation function ($G(\tau)$) in relation to a fluorescent species diffusing through a 3D Gaussian detection volume can be defined as follows:

$$G(\tau) = 1 + \frac{A}{N} \cdot \sum_{i=1}^m \cdot f_i \cdot \left(1 + \frac{\tau}{\tau_{D_i}}\right)^{-1} \cdot \left(1 + \frac{\tau}{S^2 \cdot \tau_{D_i}}\right)^{-\frac{1}{2}} \quad (1)$$

where;

$$A = 1 + \frac{T}{1-T} e^{-\tau/\tau_T} \quad (2)$$

$G(\tau)$ is the normalized intensity autocorrelation function which describes N number of fluorescent particles where f_i is the fraction of the species, i , of a total m , having a dwell time of τ_{D_i} . A is a pre-exponential factor to account for the photophysics of the fluorophore where

T which is the percentage of molecules in the triplet state and τ_T is the lifetime of the triplet state.³⁹ S is the

structure parameter that represents the ratio of the vertical to the radial axis of the confocal volume and can be determined experimentally.⁵⁴ Considering that the diffusion of the SNAP-tagged β 2AR is limited to the 2D plane of the plasma membrane, $S \rightarrow \infty$ and Equation (1) simplifies to;

$$G(\tau) = 1 + k + \frac{A}{N} \cdot \sum_{i=1}^m \cdot f_i \cdot \left(1 + \frac{\tau}{\tau_{Di}}\right)^{-1} \quad (3)$$

We used a combination of Equations (1) and (3) to model a diffusion profile to describe a first component depicting free SNAP-488 (confined to that of free SNAP-488, $\tau_{D1} = 20\text{--}80 \mu\text{s}$) and a second component that represented the membrane receptor-bound SNAP-488 (τ_{D2}). Where necessary, an offset, k , was included to allow the autocorrelation curve to be fitted with an asymptote of >1 . This is commonly seen where there is global photobleaching in the fluorescence fluctuations, for instance, due to a high immobile receptor fraction, or membrane movement within the volume, which results in a curve transposed in y . On average the offset was $0.16 \pm 0.04\%$ of the measured amplitude, reads were excluded if the offset was $> 5\%$ of the amplitude, or if an asymptotic value had not been reached. For the trace reads collected from the HEK293T lines, the initial 5 s were discarded prior to modeling to compensate for the bleaching of the fluorophore.

The precise radial and vertical axes of the confocal observation volume were determined on each experimental day by measuring the diffusion of 20 nM Rhodamine 6G as previously described.⁵⁴

Fluorescence fluctuation measurements were also analyzed using PCH (photon counting histogram) within Zen Black (2012) software. PCH analysis reports the average molecular brightness of the measured population and can be used to define whether single (one-component) or multiple brightnesses were present.⁵⁵ PCH uses a frequency distribution of photon counts within a defined time bin. A time bin of 0.1 ms was applied to all raw traces, appropriate for the diffusion speed of the membrane protein SNAP β 2AR being studied and analyzed. PCH histograms were fitted to either a one- or two-component PCH model which was determined by goodness of fit criteria at higher photons per bin values, with the data displayed on a linear-log scale. A system-dependent first-order correction was used, which accounts for photons detected outside of a true Gaussian detection volume, determined from the calibration data using Rhodamine 6G and was set at 0.3 for the Zeiss LSM510NLO ConfoCor 3 microscope and 0.6 for the Zeiss LSM880.

2.10 | Data analysis

Determination of agonist potency, antagonist affinity, and equilibrium dissociation constants were made by fitting data

within GraphPad Prism version 7 for Windows (GraphPad Software, San Diego California USA, www.graphpad.com).

Statistical significance was determined, where appropriate, using Mann-Whitney, one-way/two-way ANOVA, and Kruskal-Wallis with Tukey or Dunn's multiple comparison test if $P < .05$ (statistically significant). A minimum of three independent experiments was chosen for all experimental work. This was based on the variance of the data obtained and power analysis that predicted a high probability of observing small differences in measured parameters. For example, the probability of detecting a change in pEC₅₀ of 0.5 (3-fold) with $n = 3$ is 0.89. For $n = 4$ this increased to 0.96.

2.11 | Ligands, chemical reagents, and other materials

Streptavidin paramagnetic beads were purchased from Promega (Wisconsin, USA). Blastidin, StemPro34, Activin A, RPMI, GlutaMAX, B27, secondary antibodies, Essential 8 Medium, and the Nunc Lab-tek chambered coverglass (155411) were purchased from Thermo Fisher Scientific (Paisley, UK). BMP4 and anti-CD90 were purchased from R&D systems (Minneapolis, USA). DMEM, FBS, PBS, NEAA, trypsin, poly-D-lysine, CGP 12177, CGP 20712A, ICI 118551, propranolol, salmeterol, salbutamol, Hoechst 33342, DAPI, anti α -actinin, and formalin were purchased from Sigma-Aldrich (Missouri, USA). bFGF was purchased from PeproTech (London, UK). Matrigel (#356235) was purchased from Corning (New York, USA). Black and white 96-well plates were purchased from Greiner bio-one (Kremsmunster, Austria). Formoterol and isoprenaline were purchased from Tocris Bioscience (Bristol, UK). ³H-CGP 12177 and MicroScint 20 were purchased from PerkinElmer (Massachusetts, USA). SNAP-Surface Alexa Fluor 488 was purchased from New England Biolabs (Hitchin, UK). All other chemicals were purchased from Sigma-Aldrich.

The HUES7 cell line was a kind gift by Chad Cowan and Doug Melton.⁵¹ The BL15 was provided by David Darling.⁵⁶ The HEK293T cell line was obtained from the American Type Culture Collection (CRL-11268).

3 | RESULTS

3.1 | Characterization of ES cell progenitor cells expressing SNAP β 2AR

Relative expression levels and equilibrium dissociation constants determined from radioligand-binding with ³H-CGP 12177 were similar for the four ES progenitor cell lines expressing different haplotypes of SNAP β 2AR ($P > .05$ one-way ANOVA, Figure 1, Table 1). The non-transgenic ES

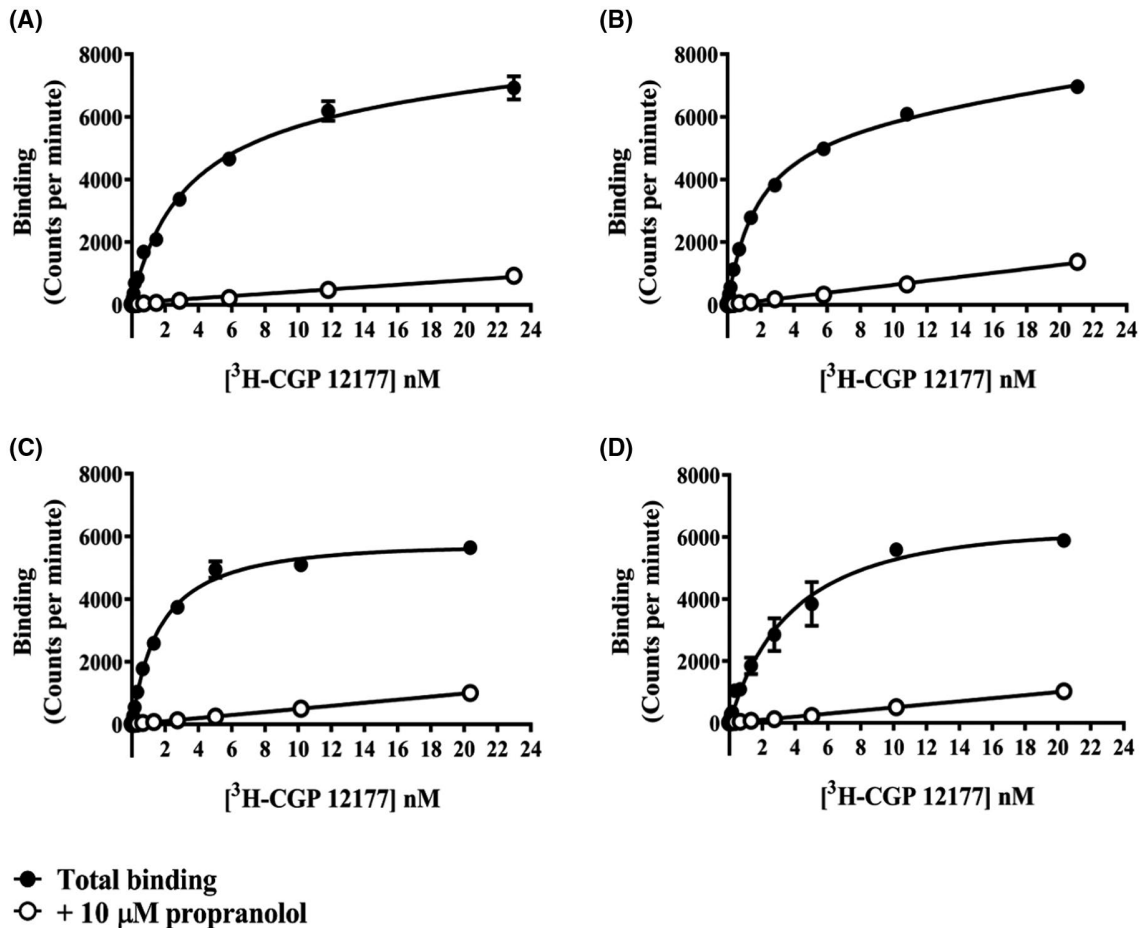


FIGURE 1 Whole-cell saturation binding of ^3H -CGP12177 in ES progenitor cell lines stably expressing SNAP β 2AR. Representative experiments demonstrating ^3H -CGP12177 binding in the presence (open circle) or absence (filled circle) of 10 μM propranolol in cells expressing the four different SNAP β 2AR haplotypes: A, Arg16Gln27 (RQ); B, Arg16Glu27 (RE); C, Gly16Gln27 (GQ) and D, Gly16Glu27 (GE). Data represent mean \pm SEM of quadruplicate determinations in a single experiment. Similar data were obtained in 3-4 separate experiments (Table 1)

cells displayed negligible-specific binding of ^3H -CGP 12177 (data not shown). Whole-cell competition binding displayed typical β 2AR pharmacology in all four ES cell lines with high affinity for propranolol, CGP 12177, and the β 2AR selective antagonist ICI 118551 and low affinity for the β 1AR selective antagonist CGP 20712A (Figure 2, Table 1). Similar results were observed when the SNAP β 2AR constructs were stably expressed in HEK293T cells (Table 1).

Confocal imaging of the SNAP β 2AR expressed within the ES cell lines showed that membrane localization of the receptor could be clearly defined and underwent agonist-induced internalization (Figure 3). A membrane-impermeable SNAP-tag substrate was used to label the receptor and therefore any intracellular receptor must have predominantly originated from the cell surface. Unstimulated ES progenitor cells expressed the SNAP β 2AR at the cell surface but there was also clear evidence of constitutive receptor internalization (Figure 3A,C). Internalized receptor appeared to exist as clustered multiple small granules in contrast to the larger clusters of merged granules observed within the transgenic HEK293T cell lines (Supporting Information Figure S2). Agonist-induced

internalization was clearly observed following 30 minutes treatment with 1 μM formoterol although high levels of receptor also remained on the cell membrane (Figure 3B,D). Very similar receptor localization was observed across the four transgenic ES cell lines in the presence and absence of the β AR agonist formoterol. Non-transgenic ES cells displayed no discernible SNAP labeling (data not shown).

3.2 | Quantitative evaluation of agonist-induced receptor internalization using high content screening

To determine agonist concentration-response relationships for ligand-induced internalization of the SNAP β 2AR, we undertook high content confocal imaging of the four haplotypes as described in Section 2.8 (Figure 4). Agonists displayed the same rank order of potency in the four ES transgenic lines with the two partial agonists salbutamol and salmeterol producing lower maximal responses than the full agonist formoterol (Table 2; Figure 4). Internalization in response to salmeterol

Haplotype	RQ	RE	GQ	GE
	pKi	pKi	pKi	pKi
<i>ES progenitor cells</i>				
Propranolol	8.37 ± 0.02 (3)	7.94 ± 0.28 (3)	8.29 ± 0.06 (4)	8.30 ± 0.06 (4)
CGP 12177	8.54 ± 0.08 (3)	8.17 ± 0.26 (3)	8.59 ± 0.06 (4)	8.49 ± 0.10 (4)
ICI 118551	8.54 ± 0.06 (3)	8.12 ± 0.16 (3)	8.34 ± 0.04 (4)	8.21 ± 0.09 (4)
CGP 20712A	5.85 ± 0.26 (3)	5.90 ± 0.18 (3)	5.82 ± 0.14 (4)	5.76 ± 0.03 (4)
<i>HEK 293T cells</i>				
Propranolol	8.44 ± 0.05 (3)	8.31 ± 0.05 (4)	8.42 ± 0.05 (4)	8.45 ± 0.03 (4)
CGP 12177	8.69 ± 0.05 (3)	8.61 ± 0.04 (4)	8.63 ± 0.08 (4)	8.67 ± 0.07 (4)
ICI 118551	8.33 ± 0.02 (3)	8.25 ± 0.05 (4)	8.37 ± 0.06 (4)	8.40 ± 0.09 (4)
CGP 20712A	5.29 ± 0.07 (3)	5.22 ± 0.16 (4)	5.75 ± 0.18 (4)	5.54 ± 0.15 (4)

TABLE 1 Binding affinities (pK_i) obtained for the four SNAP β 2AR haplotypes expressed in ES progenitor cells or HEK293T cells from inhibition of the specific binding of ^3H -CGP 12177 (0.5–1.5 nM). Determined pK_i values were not significantly different across the haplotypes ($P > .05$, 1-way ANOVA). Data are expressed as mean \pm SEM of n separate experiments. The number of separate experiments is given in parentheses. K_D values obtained for ^3H -CGP 12177 binding in each ES progenitor cell line were: RQ, 1.94 ± 0.47 nM (4); RE 3.60 ± 1.13 nM (4); GQ 2.44 ± 0.58 nM (4); GE 5.77 ± 1.87 nM (4). K_D values in HEK293T cell lines were: RQ 0.96 ± 0.12 nM (6); RE 1.11 ± 0.17 nM (6); GQ, 1.27 ± 0.22 nM (6); GE 1.77 ± 0.34 nM (6)

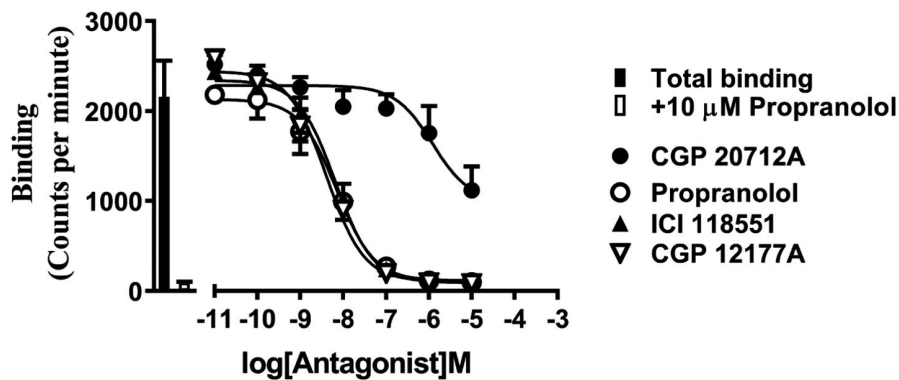


FIGURE 2 Inhibition of the binding of ^3H -CGP12177 (1 nM) by CGP 20712A (closed circles), ICI 118551 (closed triangle), CGP 12177 (open triangle), and propranolol (open circle) in ES progenitor cells expressing the Gly16Gln27 haplotype. Data represent mean \pm SEM of triplicate determinations in a single experiment. Similar results were obtained in three further experiments (Table 1)

and salbutamol was quite varied and, apart from the cell line expressing the Arg16Gln27 (RQ) haplotype of SNAP β 2AR, there were some experiments where there was no response to salbutamol, salmeterol or both (Table 2). The EC_{50} values for salmeterol and salbutamol were only determined from those experiments that produced a measurable response and these were very similar across the haplotypes (two-way ANOVA, $P > .05$). Basal levels of internalization per cell were similar across all haplotypes for the separate cell types ($P > .05$, one-way ANOVA). The internalization achieved with salbutamol was greatest for the RQ haplotype in both ES cells (Figure 4; Table 2; $P < .05$, two-way ANOVA) and HEK293T cells (Supporting Information Figure S3, Table 2).

3.3 | Reduced expression of SNAP β 2ARs following the differentiation of ES progenitor cells into fibroblasts and cardiomyocytes

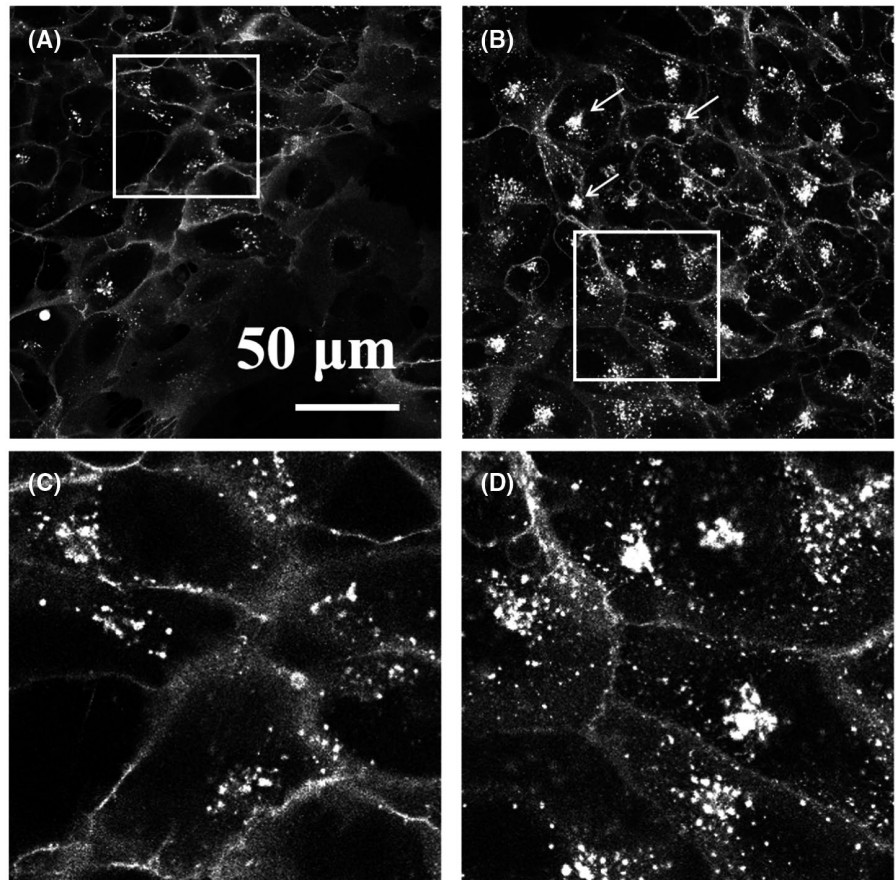
Following the differentiation of human ES cells into fibroblasts or cardiomyocytes (confirmed with the

fibroblast marker Thy-1 (CD90) and the cardiomyocyte marker α -actinin; Supporting Information Figure S1), the expression of SNAP-labeled receptors was markedly reduced (Figure 5). Only diffuse membrane labeling was observed in differentiated fibroblasts (Figure 5A–D), while SNAP β 2AR was not detectable within the CM populations using confocal imaging (Figure 5E,F). Fibroblasts did, however, display constitutive receptor internalization (Figure 5C). However, following treatment with formoterol (10 nM, 20 minutes) no major difference in the extent of membrane expression or intracellular granules was observed in the differentiated fibroblasts (Figure 5B,D).

3.4 | The use of FCS to study GPCR dynamics at low receptor expression levels

In order to quantify the expression of the SNAP β 2AR fusion protein at the cell membrane and study its dynamics in these low-expression systems, we employed fluorescence correlation spectroscopy (FCS). FCS monitors fluorescently labeled

FIGURE 3 Confocal imaging of ES progenitor cells expressing the Gly16Gln27 (GQ) SNAP β 2AR haplotype following labeling with 0.5 μ M surface-SNAP-Alexafluor488. Constitutive internalization can be observed in unstimulated cells (A) and inset (C). Increased internalization is observed following stimulation with 1 μ M formoterol, 30 minutes (B), and inset (D). Multiple intracellular granules are observed which appear to form clusters (arrows) but high membrane localization is also still observed. Images are representative of images collected from at least three independent experiments



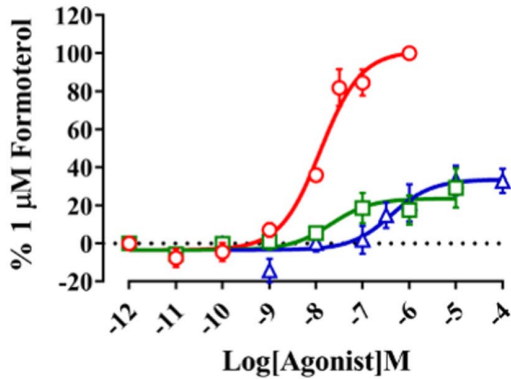
species as they pass through a small confocal volume (0.2 fl, 0.2 μ m² of membrane)⁴⁰ which can be placed within a defined region of the cell membrane. This method allows not only the quantification of such parameters as particle number per area (N/μ m²), but also provides a measurement of their average diffusion coefficient (D , μ m²s⁻¹). FCS works particularly well in low expressing systems where greater sensitivity is imparted by the larger fluctuations in fluorescence caused by low fluorescent particle numbers.⁴⁰ As a proof of principle, we optimized our protocol by studying the SNAP β 2AR in a low expression system using a CRISPR/Cas9 genome engineered HEK293T cell line that expressed the SNAP-tagged β 2AR under endogenous promotion. These data were compared with those obtained in HEK293T cells overexpressing the SNAP β 2AR following lentiviral transfection. Similar to the SNAP β 2AR in differentiated cardiomyocytes, the SNAP β 2AR within the CRISPR/Cas9 edited cells could not be visualized by standard confocal imaging (data not shown). It was possible, however, to measure fluorescence fluctuations on the cell membrane using FCS (Figure 6A). The count-rate (Hz) was 20 to 30-fold greater in the overexpressing cell line compared to the CRISPR/Cas9 genome-edited cells and this resulted in significant bleaching in the overexpression line (Figure 6B). As a consequence, the first 5 seconds of the fluctuation trace were excluded from all measurements before

the analysis of autocorrelation curves. Autocorrelation curves were constructed from these fluctuation traces (Figure 6C,D) and illustrate the difference in expression level where $G(0)$ is inversely proportional to N . Fitting of these curves showed that two distinct diffusing populations could be resolved with different dwell times in the measurement volume (Figure 6C,D). The faster-diffusing component (dwell time τ_{D1} ; 20–80 μ s) was consistent with free unbound SNAP-488 dye diffusing within the detection volume.⁴³ The slower diffusing component (τ_{D2}) represented the SNAP β 2AR expressed on the cell membrane. The diffusion coefficient (D) of this second component, however, was very similar between cell lines (Figure 6F, CRISPR: 0.12 ± 0.01 , $n = 24$; OE: 0.10 ± 0.01 μ m²s⁻¹, $n = 30$, respectively). The particle number recorded from the CRISPR/Cas9 edited cells for the SNAP β 2AR (37.4 ± 8.4 N/μ m², $n = 24$) was significantly lower than that seen in the over-expressing (OE) cells (349.1 ± 39.0 N/μ m², $n = 30$, Figure 6E, unpaired t test $P < .0001$). Fluctuations traces were then analyzed by photon counting histogram analysis (PCH) which reports the average molecular brightness of the measured population and can be used to define whether a single (one-component) or multiple brightnesses are present. An increase in brightness can indicate clustering or oligomerization of the tagged-species potentially as a result of membrane reorganization prior to GPCR internalization.⁴³ All HEK293T traces fitted

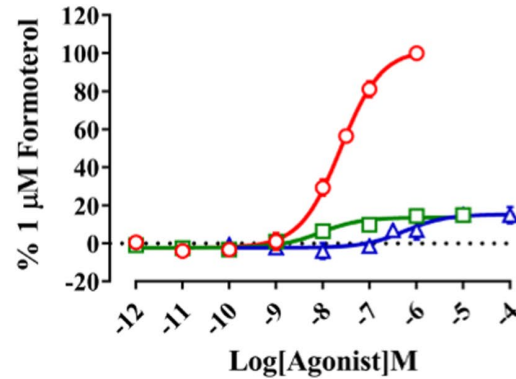
to a one-component photon counting histogram (PCH) with the overexpression (OE) cell line exhibiting a significantly higher molecular brightness (ϵ , counts per molecule (cpm)

per second; Supporting Information Figure S4, CRISPR: $20\,728 \pm 2730$ cpm.s⁻¹, $n = 24$; OE: $34\,620 \pm 3322$ cpm.s⁻¹, $n = 30$; $P < .01$ un-paired t test).

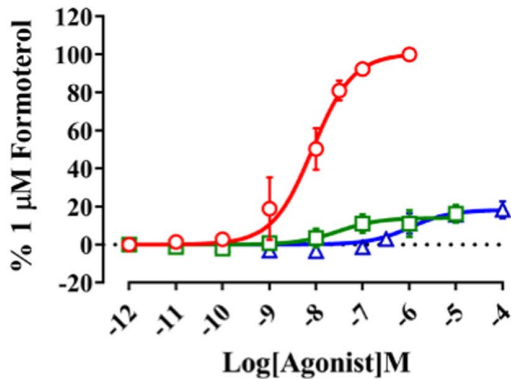
(A) RQ



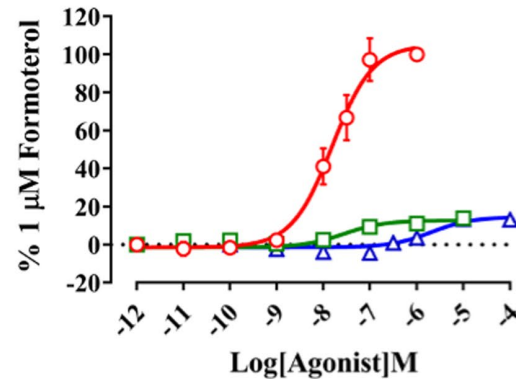
(B) RE



(C) GQ

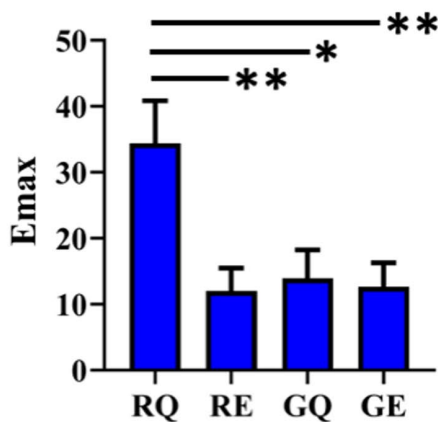


(D) GE



○ Formoterol
□ Salmeterol
△ Salbutamol

(E) Salbutamol



(F) Salmeterol

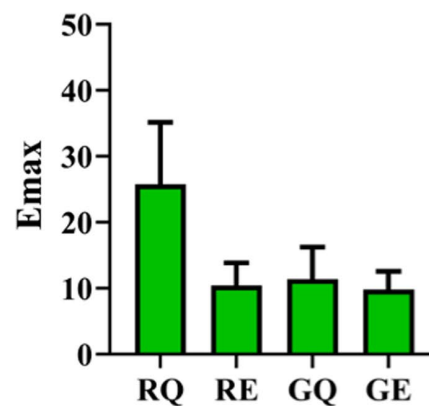


FIGURE 4 Quantification of agonist-induced internalization of SNAP β 2AR in ES progenitor cells expressing the four different haplotypes: A, Arg16Gln27 (RQ); B, Arg16Glu27 (RE); C, Gly16Gln27 (GQ) and D, Gly16Glu27 (GE). A-D, Single experiments ($n = 6-9$) were performed with duplicate determinations and plotted data represent mean \pm SEM of the number of SNAP-488 labeled granules expressed as a percentage of that obtained with 1 μ M formoterol after 1 hour stimulation with β AR agonists; formoterol (red circle), salmeterol (green square) and salbutamol (blue triangle). EC₅₀ and E_{MAX} values alongside the number of separate experiments performed are provided in Table 2. Derived Emax values (mean \pm SEM, $n = 6-9$) for salbutamol (E, blue) and salmeterol (F, green) are also shown. Raw data were subject to 2-way ANOVA with Tukey's multiple comparison test; * $P < .05$, ** $P < .01$

3.5 | FCS measurements in ES progenitor cells and ES-derived fibroblasts and cardiomyocytes

The use of FCS in human ES cells and derived cell types required additional steps to locate the cell membrane (Figure 7). Typically the upper membrane of a cell expressing a SNAP-labeled membrane receptor can be identified as the peak of a z-intensity scan; however, this was not the case for the ES and derived cell types. The non-uniform nature of these cells coupled with the short sampling time meant that fluctuation traces which most closely described the apical membrane could be located up to 1 μ m above this peak. Primary cells are routinely non-uniform and in the case of the cells, we have studied here, very thin. While the waist of the confocal volume is around 0.25 μ m in diameter the vertical axial range is closer to 1 μ m. A confocal volume, therefore, placed on a thin primary cell could theoretically encompass both apical and basal membranes. To ensure we could capture the trace that most closely represented that of the apical membrane we took sequential 20-30 seconds trace reads every 0.25 μ m through the cell starting above the cell membrane (Figure 7B,D). The first trace showing clear membrane-related fluctuations was used to determine membrane diffusion properties of the receptor. Two distinct decay populations could be resolved relating to the SNAP-488 within these progenitor cells similar to those observed in HEK293T cells (Figure 7E).

Single point FCS was carried out on ES progenitor cells, differentiated ES-derived fibroblasts, and ES-derived cardiomyocytes expressing the GQ variant of SNAP β 2AR to determine relative membrane particle number and diffusion properties of the SNAP β 2AR (Figure 8). Fluorescence fluctuations could be detected in all three cell types and traces representing the apical membrane could be readily identified (Figure 8A-C). Two distinct diffusing species could be detected in all three transgenic cell types (Figure 8D-F). The drop in receptor expression level observed using confocal microscopy was confirmed using FCS where the average particle number recorded from the ES-GQ cells (186.8 ± 33.2 N/ μ m², $n = 14$) was significantly greater than that seen in differentiated GQ fibroblasts (60.6 ± 10.9 N/ μ m², $n = 28$) and GQ cardiomyocytes (26.1 ± 4.6 N/ μ m², $n = 23$) (Figure 8G, Kruskal-Wallis, fibroblasts $P < .01$, cardiomyocytes $P < .0001$). The diffusion coefficients (D) were, however, very similar between cell types (Figure 8H; ES cells, 0.054 ± 0.005 μ m²s⁻¹ ($n = 14$); fibroblasts, 0.055 ± 0.004

μ m²s⁻¹ ($n = 28$) and cardiomyocytes, 0.052 ± 0.005 μ m²s⁻¹ ($n = 23$); Kruskal-Wallis, $P > .05$). The majority of traces, from all cell types (ES; 92.9%, fibroblasts; 75%, cardiomyocytes; 95.7%), fitted to a one-component fit with a brightness consistently $<16\ 000$ cpm.s⁻¹ (Figure 8I). The minority of traces fitted to a multiple component fit consisting of two distinct brightnesses, the first being $<16\ 000$ cpm.s⁻¹ and the second being $>16\ 000$ cpm.s⁻¹ (Figure 8I). The average molecular brightness (ϵ) was unaffected (Figure 8I; ES cells 6577 ± 920 cpm.s⁻¹ ($n = 14$); fibroblasts 5197 ± 396 cpm.s⁻¹ ($n = 28$); cardiomyocytes 6074 ± 866 cpm.s⁻¹ ($n = 23$); Kruskal-Wallis, $P > .05$).

3.6 | Monitoring receptor internalization using FCS

While high-content imaging provides a powerful methodology to study agonist-internalization of SNAP β 2ARs in cells, FCS analysis allowed us to investigate the effect of an agonist in a membrane micro-domain of single living cells. ES-derived fibroblasts did not show agonist-induced internalization when monitored using confocal microscopy. To confirm this finding we undertook FCS studies on ES-derived fibroblasts using the SNAP β 2AR-RQ haplotype. The RQ haplotype was chosen since it consistently responded to agonist challenge with the highest level of receptor internalization in ES progenitor cells (Figure 4). In keeping with the observations made using confocal microscopy (Figure 5), agonist treatment (10 minutes, 10 nM formoterol) had no significant effect on SNAP β 2AR-RQ particle number (N/ μ m²) in ES-derived fibroblasts (Figure 9A, Control; 173.2 ± 23.8 , $n = 21$. Formoterol; 150.3 ± 24.6 , $n = 22$, Mann-Whitney, $P > .05$). The diffusion coefficient (D, μ m²s⁻¹) was also unaffected by agonist treatment (Figure 9B. Control, 0.041 ± 0.003 , $n = 21$; Formoterol, 0.043 ± 0.004 , $n = 22$, Mann-Whitney, $P > .05$). Finally, the traces were also subject to PCH analysis to determine the average molecular brightness (ϵ). All traces fitted to a one-component PCH with no significant change observed following formoterol treatment (Figure 9C, Control; 6939 ± 891 cpm.s⁻¹, $n = 21$. Formoterol; 6901 ± 633 cpm.s⁻¹, $n = 22$).

To confirm that we were able to observe agonist-induced changes in the parental ES progenitor cells within

TABLE 2 Agonist potencies (pEC_{50}) and maximal responses (E_{max}) obtained for formoterol, salbutamol and salmeterol-mediated production of intracellular granules as a measure of agonist-induced internalization. If wells did not respond to agonist, E_{max} was set to zero and data were not included in pEC_{50} calculations. E_{max} values are expressed as a percentage of the response obtained with 1 μM formoterol. Data are expressed as mean \pm SEM of n separate experiments. The number of separate experiments is given in parentheses. Determined pEC_{50} values were not significantly different across the haplotypes for either cell type ($P > .05$, 2-way ANOVA). The determined E_{max} value following salbutamol treatment was significantly increased in the ES RQ haplotype ($*P < .05$ or $**P < .01$, 2-way ANOVA with Tukey's multiple comparison test) compared to that in the other haplotypes. The determined E_{max} value following salbutamol treatment was significantly decreased in the HEK 293T GE haplotype compared to the RQ and GQ haplotypes ($*P < .05$, 2-way ANOVA with Tukey's multiple comparison test)

Haplotype	RQ		RE		GQ		GE	
	pEC_{50}	E_{MAX}	pEC_{50}	E_{MAX}	pEC_{50}	E_{MAX}	pEC_{50}	E_{MAX}
<i>ES progenitor cells</i>								
Formoterol	7.87 \pm 0.06 (7)	102.6 \pm 3.3 (7)	7.66 \pm 0.06 (11)	101.2 \pm 2.0 (11)	8.13 \pm 0.26 (8)	105.1 \pm 1.2 (8)	7.75 \pm 0.15 (8)	109.4 \pm 4.6 (8)
Salbutamol	6.29 \pm 0.30 (7)	34.4 \pm 6.5 (7)	6.06 \pm 0.15 (8)	12.0 \pm 3.5** (11)	5.99 \pm 0.19 (6)	13.9 \pm 4.3* (8)	5.79 \pm 0.06 (7)	12.6 \pm 3.7** (8)
Salmeterol	7.43 \pm 0.31 (7)	25.8 \pm 9.4 (7)	7.69 \pm 0.38 (7)	10.4 \pm 3.4 (11)	7.32 \pm 0.63 (5)	11.4 \pm 4.8 (8)	7.40 \pm 0.25 (6)	9.8 \pm 2.8 (8)
<i>HEK 293T cells</i>								
Formoterol	8.34 \pm 0.04 (7)	103.3 \pm 1.9 (7)	8.44 \pm 0.09 (9)	100.9 \pm 1.5 (9)	8.48 \pm 0.10 (7)	102.6 \pm 2.0 (7)	8.31 \pm 0.11 (6)	108.3 \pm 3.4 (6)
Salbutamol	6.39 \pm 0.08 (7)	53.9 \pm 6.0* (7)	6.29 \pm 0.17 (9)	45.9 \pm 5.6 (9)	6.21 \pm 0.18 (7)	55.4 \pm 2.3* (7)	6.26 \pm 0.11 (6)	38.0 \pm 4.1 (6)
Salmeterol	8.30 \pm 0.11 (6)	25.6 \pm 5.4 (7)	8.21 \pm 0.27 (7)	20.4 \pm 5.3 (9)	8.15 \pm 0.24 (7)	28.2 \pm 1.5 (7)	8.08 \pm 0.21 (6)	16.9 \pm 2.0 (6)

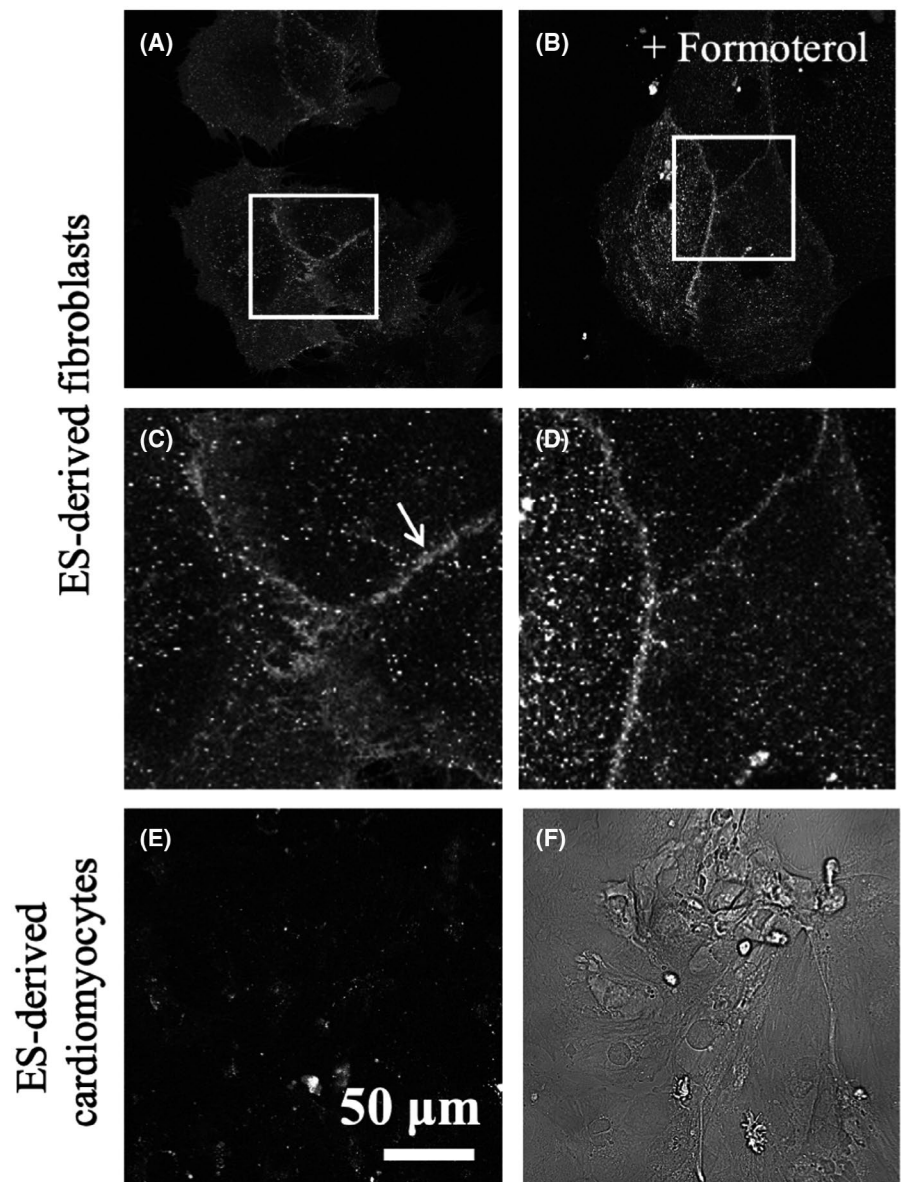
the membrane using single point FCS, we studied the ES-SNAP β 2AR-RQ progenitor cell line which exhibited agonist-induced internalization using both confocal imaging and high content imaging (Figures 3 and 4). ES-SNAP β 2AR-RQ cells subject to formoterol treatment (10 minutes, 10 nM formoterol) displayed significantly reduced SNAP β 2AR particle numbers (Figure 9D, 143.8 ± 23.1 N/ μm^2 , $n = 27$) compared to those treated with vehicle (341.9 ± 60.0 N/ μm^2 , $n = 27$. Mann-Whitney, $P < .01$). The diffusion coefficient (D , $\mu m^2 s^{-1}$) of the SNAP β 2AR was, however, not affected by agonist treatment (Figure 9E; control, 0.045 ± 0.004 , $n = 27$; formoterol treatment, 0.039 ± 0.003 , $n = 27$). In contrast, the molecular brightness (ϵ) of all traces fitted to a one-component PCH and was significantly increased following formoterol treatment (Figure 9F; control; 3061 ± 415 cpm. s^{-1} , $n = 26$; formoterol, 4121 ± 531 cpm. s^{-1} , $n = 27$. $P > .05$). These data suggest that the SNAP β 2AR-RQ is clustering on the cell membrane in ES progenitor cells prior to internalization following agonist treatment.

The particle number in ES-derived fibroblasts, under control conditions, appeared to be dependent on haplotype, GQ (Figure 8; 60.61 ± 10.89 N/ μm^2 , $n = 28$) being lower than that of RQ (Figure 9; 173.2 ± 23.8 N/ μm^2). In order to check that the lack of internalization in ES-derived fibroblasts was not due to haplotype, we undertook a second series of experiments in ES-derived fibroblasts expressing the GQ haplotype (Figure 9G-I). Particle number was of a similar order to that previously measured, reduced compared to that observed in the RQ ES-derived fibroblasts and not significantly affected by formoterol treatment (Figures 9G and 10; control, 99.7 ± 15.1 , $n = 20$; formoterol, 128.0 ± 15.1 N/ μm^2 , $n = 19$; $P > .05$). This was also the case for the molecular brightness (control; 4803 ± 374 cpm. s^{-1} , $n = 20$; formoterol, 5876 ± 653 cpm. s^{-1} , $n = 19$; $P > .05$) and diffusion coefficient (control; 0.040 ± 0.004 , $n = 20$; formoterol, 0.048 ± 0.005 $\mu m^2 s^{-1}$, $n = 19$; $P > .05$).

4 | DISCUSSION

In the present study, we have used a combination of FCS and ES cell technology to investigate the impact of cell differentiation on receptor mobility and internalization in human ES progenitor cells and in ES-derived cardiomyocytes and fibroblasts. We generated four different ES progenitor cells expressing SNAP-tagged β_2 -adrenoceptors with one of the four haplotypes involving single-nucleotide polymorphisms at position 16 (arginine or glycine) and position 27 (glutamine or glutamate). All expressed the SNAP β 2AR to a similar level and all four haplotypes could be internalized in response to the full agonist formoterol, as determined by high content confocal imaging. Salmeterol and salbutamol acted as partial agonists for this response, and in the case

FIGURE 5 Confocal imaging of SNAP β 2AR in (A-D) human ES-derived fibroblasts expressing the Arg16Glu27 haplotype or (E,F) human ES-derived cardiomyocytes expressing the Arg16Gln27 haplotype. All cells were labeled with 0.5 μ M surface-SNAP-Alexafluor488. E, No visible SNAP labeling could be observed through standard confocal imaging of ES-derived cardiomyocytes; F, brightfield image is included to illustrate the presence of cells. While SNAP β 2AR could be imaged in ES-derived fibroblasts (A) and inset (C) it was not possible to identify agonist-induced internalization of receptor following formoterol (10 nM; 20 minutes) treatment (B, and inset (D)). A-D, Diffuse membrane expression could be observed, more strongly apparent at membrane-membrane boundaries (arrow).



of salbutamol, there was a significantly greater internalization in the RQ (Arg16Gln27) expressing cells compared to cells expressing the other three haplotypes. Positions 16 and 27 are both within the extracellular N-terminal region of the receptor that has been implicated in the regulation of receptor recycling and down-regulation.¹⁷⁻²⁰ In agreement with the data presented here, previous *in vivo* cardiovascular experiments in human volunteers have linked the RQ haplotype with enhanced receptor desensitization, while the GE haplotype produces a blunted susceptibility to agonist-induced desensitization.^{57,58}

A striking feature of the initial experiments performed with ES-derived cardiomyocytes and fibroblasts was that the expression of SNAP-tagged β_2 -adrenoceptors dropped dramatically following the differentiation process. Although the receptor was still detectable in ES-derived fibroblasts, this was not the case with ES-derived cardiomyocytes where the

SNAP β 2AR fluorescence could not be distinguished from background autofluorescence. One approach that has the sensitivity to monitor receptors in membrane microdomains at very low receptor expression levels is FCS.⁴⁰ FCS monitors fluorescently labeled species as they pass through a small confocal volume (0.2 fl, 0.2 μ m² of membrane)⁴⁰ and allows the quantification of receptor expression in terms of fluorescent particle number (N/μ m²) and their diffusion characteristics (D, μ m²s⁻¹). FCS works particularly well in low expressing systems where greater sensitivity is imparted by the larger statistical variation caused by low fluorescent particle numbers.⁴⁰ As a consequence, the autocorrelation function $G(\tau)$ at $\tau = 0$ is inversely proportional to the particle number.⁴⁰

As a first step to apply FCS to study cell surface receptor expression in membrane microdomains of single ES-derived cells, we undertook a comparison of SNAP-tagged β_2 -adrenoceptors in HEK293T cells overexpressing

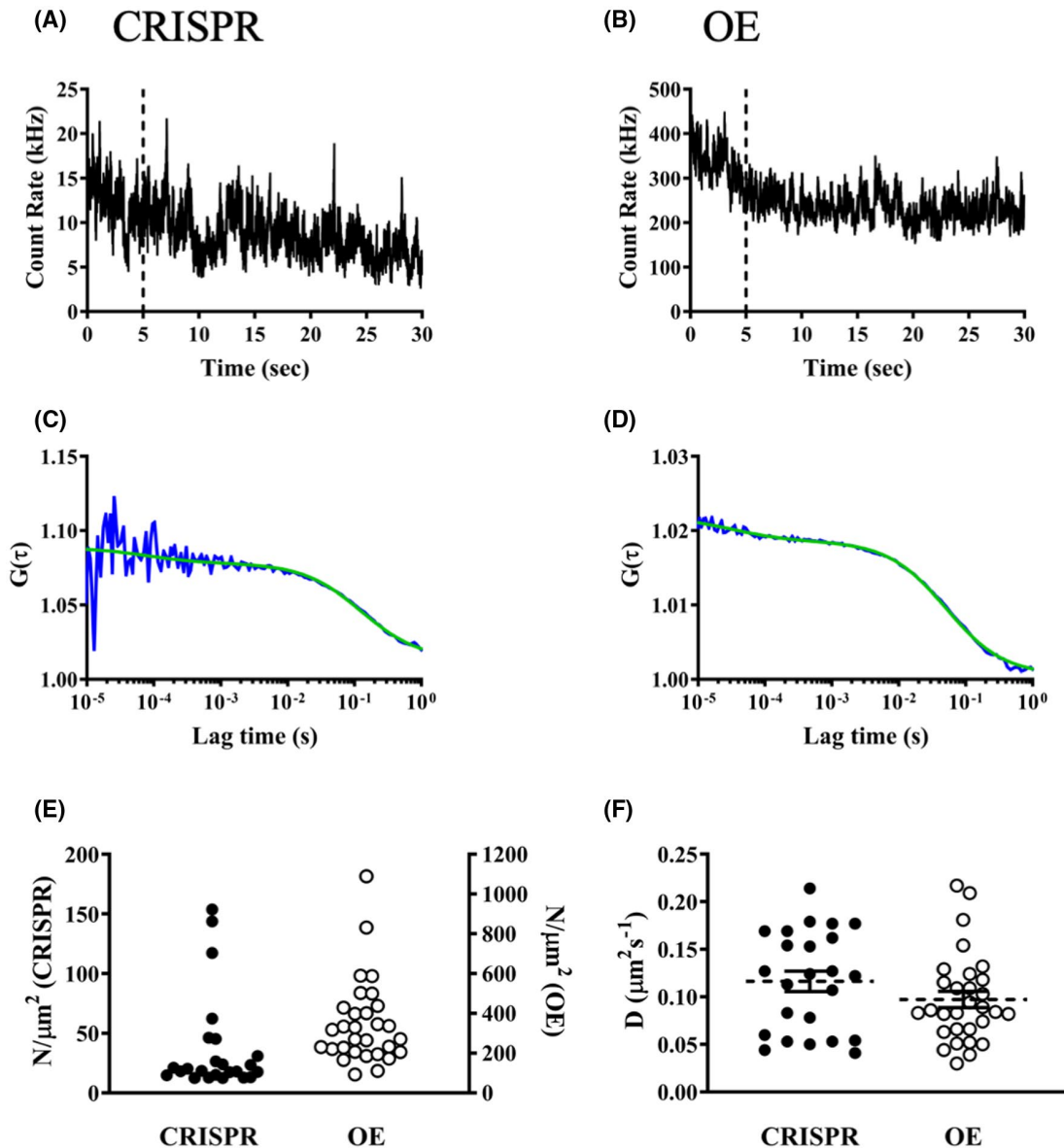


FIGURE 6 Fluorescence correlation spectroscopy of CRISPR/Cas9 edited HEK293T cells. Representative FCS traces taken on the cell membrane of (A) HEK293T cells that have been CRISPR/Cas9 genome-engineered to express SNAP β 2AR under endogenous promotion or (B) HEK293T cells overexpressing (OE) SNAP β 2AR. C, Autocorrelation analysis for CRISPR/Cas9 genome-edited cells and (D) OE cells. Raw (blue) and fitted data (green) are displayed. E, Individual mean particle number $N/\mu\text{m}^2$ and (F) diffusion coefficient (D ; $\mu\text{m}^2\text{s}^{-1}$) measurements are plotted for CRISPR (closed circles) and OE (open circles) cell lines. In (E) please note the different scales for the CRISPR and OE particle numbers. In (F) the mean \pm SEM of all measurements (dotted line) are displayed for each cell line

SNAP β 2AR following lentivirus transfection or in CRISPR/Cas9 genome-edited HEK293T cells expressing SNAP β 2AR under endogenous promotion. In HEK293T cells, the endogenous expression of β_2 -adrenoceptors is very low⁵⁹ and SNAP β 2ARs were not detectable by confocal microscopy in CRISPR/Cas9 genome-edited HEK293T cells. The use of FCS was, however, able to detect the large difference in expression levels (CRISPR cells, 37.4 particles per μm^2 ; lentivirus over-expressing cells, 349.1 particles per μm^2) without a significant difference in the diffusion coefficient of the β_2 -adrenoceptor between the two cell types. Interestingly, the average molecular brightness of the diffusing fluorescent

particles containing SNAP β 2ARs in over-expressing cells was significantly higher than that in the CRISPR/Cas9 genome-edited cells. This perhaps indicates that the clustering of the β_2 -adrenoceptor is occurring at higher expression levels similar to the observation recently made for CXCR4, which forms transient homodimers at high receptor densities.⁶⁰ The difference in brightness of SNAP β 2ARs between overexpressed cells and CRISPR/Cas9 genome-edited HEK293 cells is approximately twofold. It has been previously reported that β_2 -adrenoceptors have a propensity to form dimers and higher order oligomers³⁶ but at the present time, we cannot conclude whether the changes observed for

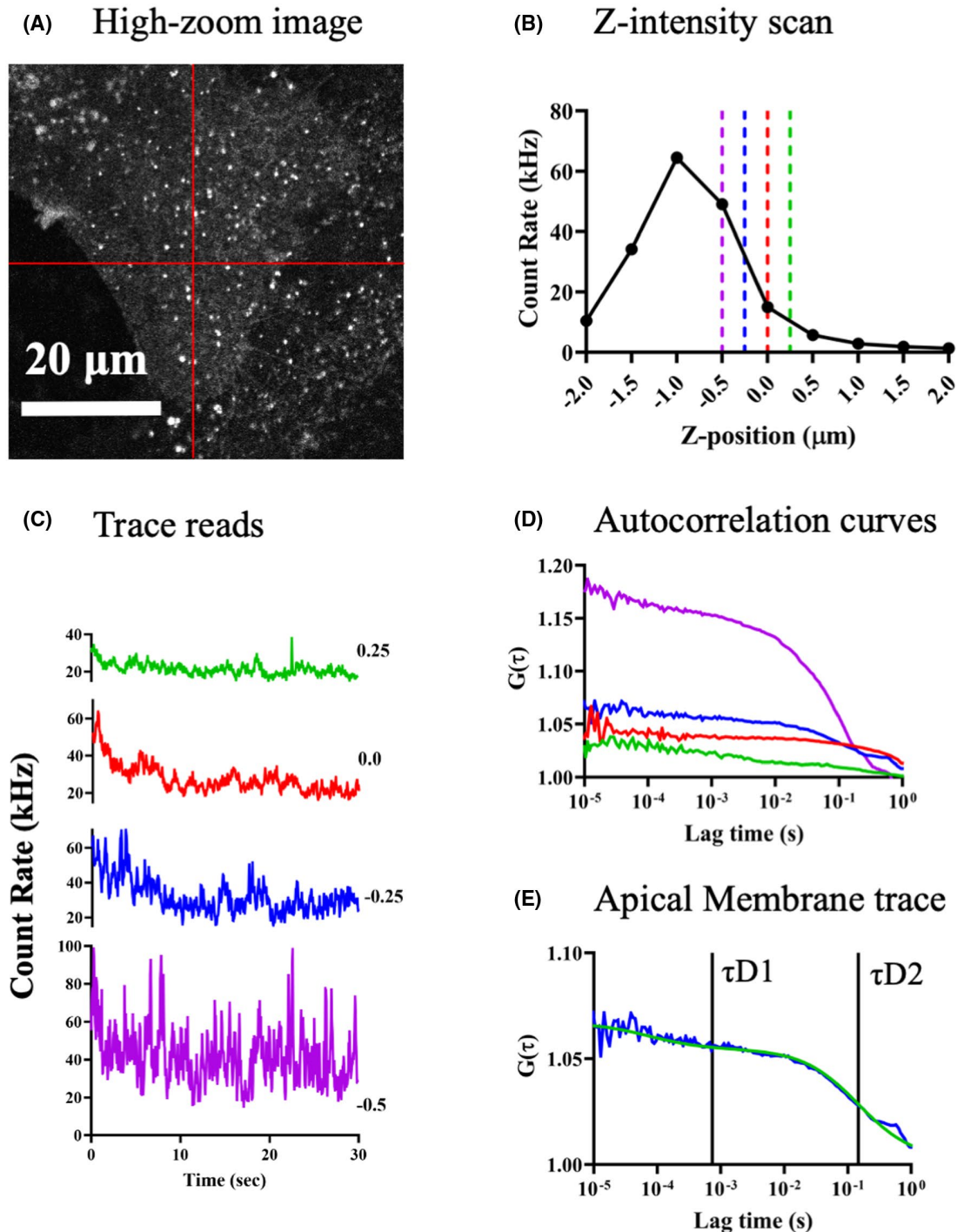


FIGURE 7 Positioning the confocal volume on the cell membrane of ES or differentiated cell type. A, The FCS detection volume, depicted by the red crosshair intersect, is positioned on the live high-zoom confocal image of an ES-derived fibroblast expressing the Gly16Gln27 haplotype of SNAP β 2AR labeled with 0.1 μ M surface-SNAP AlexaFluor488. The z-position of the upper membrane is approximated by eye, and bright clusters are avoided as these could represent immobile receptor. B, An intensity z-scan is recorded at low laser power at the crosshair, at 2 μ m above and below the approximated position of the upper cell membrane (position 0.0 μ m) in 0.5 μ m steps. The FCS detection volume is moved to +1.5 μ m above the peak intensity reading (eg, moved to position 0.5 μ m). C, 1 \times 30 seconds FCS trace reads are collected at experimental laser power every 0.25 μ m moving toward the position of peak intensity. FCS trace reads obtained at the z positions displayed in (B) are shown. D, Autocorrelation curves are constructed for individual traces within Zen Black (2012) software. Curves are modeled with a 1 \times 3D + 1 \times 2D autocorrelation model which includes a triplet component and an offset to allow for membrane drift (see Section 2.9). Curves can be excluded for several reasons, including if the 2D component is too fast/slow to depict a membrane protein (purple trace), if the curve fails to reach a lower plateau or allowed offset is too great (red trace), or if the curve cannot be described by the model. The blue and green traces contain a membrane component; however, the blue trace is selected as this trace has a greater proportion of 2D vs 3D fluctuations. E, Autocorrelation curve and model for the selected blue trace. The 3D dwell time, τ_{D1} = 74 μ s and represents free surface-SNAP-AlexaFluor488, the 2D dwell time, τ_{D2} = 146 ms and represents SNAP labeled SNAP β 2AR. Blue—raw data, green—fit model

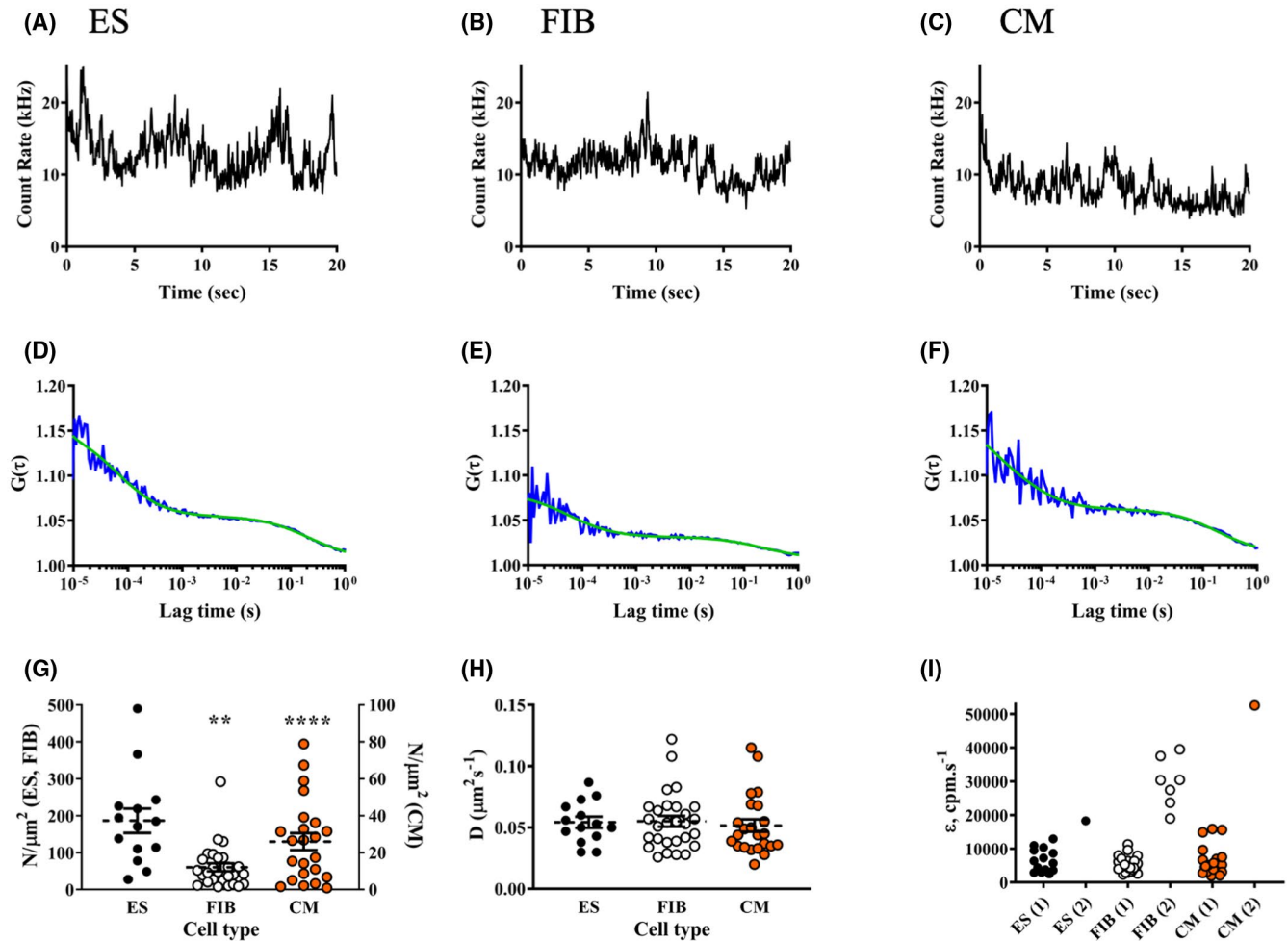


FIGURE 8 Cell membrane fluorescence correlation spectroscopy of human ES progenitor cells and differentiated fibroblasts and cardiomyocytes. Representative traces are shown for (A) ES progenitor cells, (B) ES-derived fibroblasts, and (C) ES-derived cardiomyocytes expressing the SNAP β 2AR with the Gly16Gln27 haplotype. Autocorrelation traces (blue) and the resulting autocorrelation fit (green) are shown for (D) ES progenitor cells, (E) fibroblasts, and (F) cardiomyocytes. Individual experimental (G) membrane particle number $N/\mu\text{m}^2$, (H) diffusion coefficients D ($\mu\text{m}^2\text{s}^{-1}$) and (I) molecular brightness ϵ , (cpm. s^{-1}), are plotted with the mean (dotted line) \pm SEM for ES (black closed circles), FIB (black open circles) and CM (orange closed circles). G, Average particle number recorded for ES progenitor cells is significantly greater than that recorded in ES-derived fibroblasts ($P < .01$) and ES-derived cardiomyocytes ($P < .0001$; Kruskal-Wallis). I, data were fitted to either a one-component or two-component PCH analysis and the first (1, left) and second (2, right) brightness values are plotted. For data that fit to a two-component analysis the second, brighter, population represented a small percentage of the total measured population; 5.1% (ES; $n = 1$), 5.7% (CM, $n = 1$) and $3.1\% \pm 0.9$ (FIB, $n = 7$)

the β_2 -adrenoceptor reflect changes in monomer-dimer or dimer-higher-oligomer equilibria.

FCS was able to quantify the large difference in β_2 -adrenoceptor expression levels between ES progenitor cells expressing the Gly16Gln29 (GQ) haplotype (186.8 particles per μm^2) and the equivalent ES-derived GQ fibroblasts (60.6 particles per μm^2) and ES-derived GQ cardiomyocytes (26.1 particles per μm^2). Diffusion coefficients were similar across all three ES cell lines ($0.05 \mu\text{m}^2\text{s}^{-1}$) and approximately half the value of the diffusion coefficients obtained in HEK293T cells ($0.1 \mu\text{m}^2\text{s}^{-1}$) indicative of their different membrane compositions and organizations. The particle number detected by FCS in ES-progenitor cells expressing the Arg16Gln27 (RQ) phenotype (341.9 particles per μm^2) was higher than

in the equivalent GQ cells and following differentiation to ES-derived fibroblasts, the particle number (173.2 particles per μm^2) was also higher than that detected in the equivalent GQ haplotype, but significantly lower than in the (RQ) ES-progenitor cells.

The RQ haplotype was chosen for studies of agonist-induced receptor internalization of SNAP β 2ARs using FCS since it consistently exhibited a robust agonist-induced receptor internalization in ES progenitor cells when monitored by high content confocal imaging.

Following agonist treatment of ES progenitor cells (10nM formoterol, 10 minutes), the SNAP β 2AR-RQ haplotype displayed a significant reduction in cell surface particle number from 341.9 particles per μm^2 to 143.8 particles per μm^2

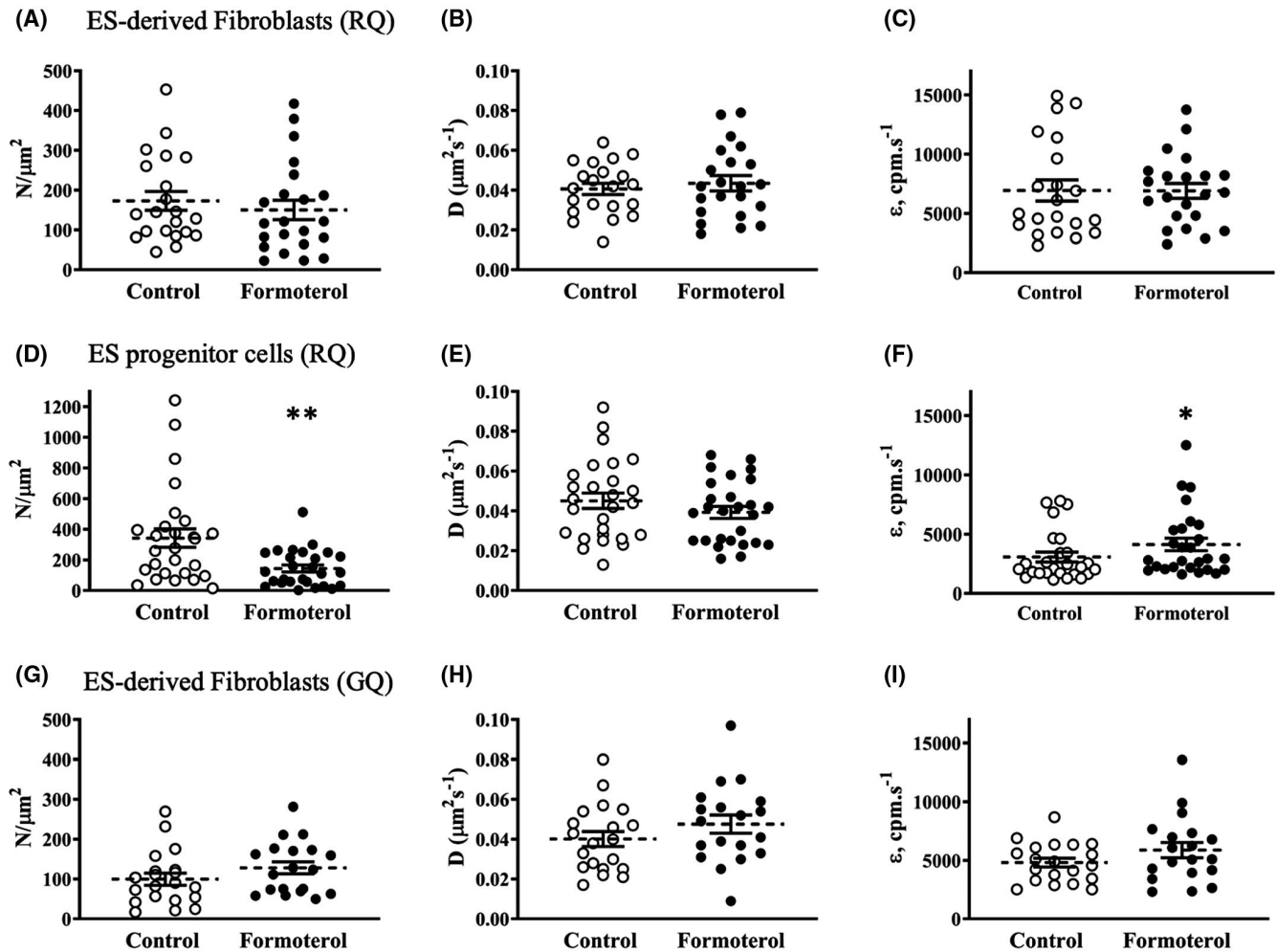


FIGURE 9 Fluorescence correlation spectroscopy to study the effect of formoterol (10 nM, 10 minutes) on ES-derived fibroblasts (A-C) and ES progenitor cells (D-F) expressing the Arg16Gln27 (RQ) haplotype of the SNAP β 2AR. Also shown are data for ES-derived fibroblasts expressing the Gly16Gln27 (GQ) haplotype (G-I). Data show particle number (A, D, G), diffusion coefficient (B, E, H), and molecular brightness (C, F, I). Measurements were made in the presence (black closed circles) or absence (black open circles) of formoterol (10 nM, 10 minutes). Grouped mean values (dotted line) \pm SEM are also shown. $P < *.05$ and $**.01$, Kruskal-Wallis test

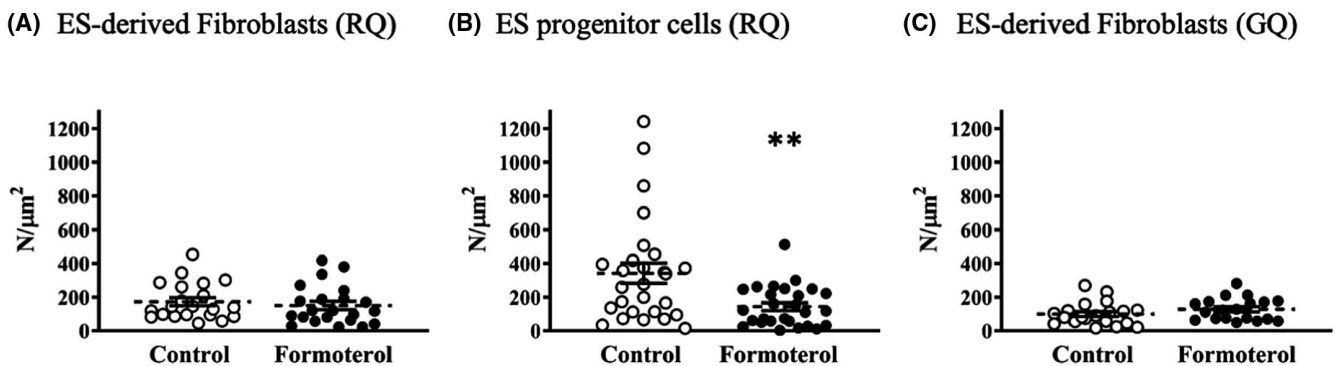


FIGURE 10 Particle number data from Figure 9 are displayed on the same scale to allow comparison. Particle number, as determined by Fluorescence Correlation Spectroscopy, for ES-derived fibroblasts (A) and ES progenitor cells (B) expressing the Arg16Gln27 (RQ) haplotype and (C) ES-derived fibroblasts expressing the Gly16Gln27 (GQ) haplotype of the SNAP β 2AR. Measurements were made in the presence (black closed circles) or absence (black open circles) of formoterol (10 nM, 10 min). Grouped mean values (dotted line) \pm SEM are also shown. $P < *.05$ and $**.01$, Kruskal-Wallis test

which was consistent with agonist-induced receptor internalization. The diffusion coefficients of the receptor-containing complexes were not affected by agonist treatment but their molecular brightness (ϵ) was significantly increased, suggesting that there maybe clustering of β_2 -adrenoceptor on the cell membrane prior to internalization. It is notable that the brightness values observed in ES progenitor cells (and also fibroblasts and cardiomyocytes) were very much lower than those measured in HEK293 cells and this probably reflects the impact of the local cellular environment and fluorescence quenching. The role of receptor clustering on the cell membrane has been reported previously in association with the internalization of particular GPCRs including the β_2 -adrenoceptor^{43,61} and the 1.35-fold increase in brightness observed in ES progenitor cells probably equates to an increase in the proportion of dimeric/oligomeric species as receptors are sequestered at sites of receptor endocytosis.

In marked contrast to the data obtained in ES progenitor cells, no significant reduction in particle number was evident in ES-derived fibroblasts following formoterol treatment in cells expressing either the Arg16Gln27 (RQ) or Gly16Gln27 (GQ) haplotypes. These data were, however, consistent with the observations made in ES-derived fibroblasts expressing the RQ haplotype using confocal microscopy (Figure 5). Taken together these studies indicate that susceptibility to agonist-induced receptor internalization is dependent upon cell phenotype and can be changed following the differentiation of ES progenitor cells into fibroblasts. This may have important implications for drug discovery where attempts are being made to introduce signaling bias into agonist molecules that can stabilize specific conformations of GPCRs and alter their ability to couple to G proteins or β -arrestin molecules.⁶² Reduced internalization will reduce the extent of signaling from intracellular endosomes.^{10,11} Furthermore, the differential sensitivity of different cell phenotypes to agonist-induced internalization of the β_2 -adrenoceptor may also have implications for drug therapy with inhaled long-acting β_2 -agonists.^{63,64}

In summary, the present study has demonstrated the power of FCS in investigating cell surface β_2 -adrenoceptors at the very low expression levels often seen in endogenously expressing cells. FCS was able to detect SNAP-tagged β_2 -adrenoceptor expression in both ES-derived cardiomyocytes and CRISPR/Cas9 genome-edited HEK293T cells, where the expression level was too low to detect them using standard confocal microscopy. Furthermore, the use of ES cell technology in combination with FCS allowed us to demonstrate that cell surface β_2 -adrenoceptors can be internalized in response to formoterol-stimulation in ES progenitor cells but not following their differentiation into ES-derived fibroblasts. This indicates that the process of agonist-induced receptor internalization is strongly influenced by cell phenotype and

this may have important implications for drug treatment with long-acting β_2 -agonists.

ACKNOWLEDGMENTS

This project was funded by the Medical Research Council [grant numbers G0800006, MR/N020081/1] and British Heart Foundation [grant number RG/14/1/30588]. CWW is supported by an NHMRC CJ Martin Fellowship (1088334) and by a UWA fellowship support grant. We wish to thank Yorick Guerout for technical assistance. We thank the School of Life Sciences imaging facility (SLIM) and staff for their contribution to this publication.

CONFLICT OF INTEREST

The applicants declare no conflicts of interest.

AUTHOR CONTRIBUTIONS

S.J. Hill, C. Denning, A. Kondrashov, J. Goulding, and S.J. Briddon conceived and designed the research study; J. Goulding, A. Kondrashov, S.J. Mistry, T. Melarangi, N.T.N. Vo, D.M. Hoang, C.W. White performed the research; J. Goulding, S.J. Mistry analyzed the data; J. Goulding, A. Kondrashov, C. Denning, S.J. Briddon, S.J. Hill wrote the manuscript. All authors contributed to the final editing of the manuscript.

ORCID

Joëlle Goulding  <https://orcid.org/0000-0002-6227-4483>

Alexander Kondrashov  <https://orcid.org/0000-0003-3428-5975>

Carl W. White  <https://orcid.org/0000-0002-4975-6189>

Chris Denning  <https://orcid.org/0000-0003-0802-8617>

Stephen J. Briddon  <https://orcid.org/0000-0001-8514-0827>

<https://orcid.org/0000-0001-8514-0827>

<https://orcid.org/0000-0001-8514-0827>

REFERENCES

- Hilger D, Masureel M, Kobilka BK. Structure and dynamics of GPCR signaling complexes. *Nat Struct Mol Biol.* 2018;25:4-12.
- Rasmussen SG, DeVree BT, Zou Y, et al. Crystal structure of the β_2 adrenergic receptor-Gs protein complex. *Nature.* 2011a;477:549-555.
- Rasmussen SG, Choi HJ, Fung JJ, et al. Structure of a nanobody-stabilized active state of the $\beta(2)$ adrenoceptor. *Nature.* 2011b;469:175-180.
- Ring AM, Manglik A, Kruse AC, et al. Adrenaline-activated structure of β_2 -adrenoceptor stabilized by an engineered nanobody. *Nature.* 2013;502:575-579.
- Masureel M, Zou Y, Picard LP, et al. Structural insights into binding specificity, efficacy and bias of a β_2 AR partial agonist. *Nat Chem Biol.* 2018;14:1059-1066.
- Kobilka B. Adrenergic receptors as models for G Protein-coupled receptors. *Annu Rev NeuroSci.* 1992;15:87-114.
- Violin JD, Ren XR, Lefkowitz RJ. G protein-coupled receptor kinase specificity for β -arrestin recruitment to the β_2 -adrenergic

- receptor revealed by fluorescence resonance energy transfer. *J Biol Chem.* 2006;281:20577-20588.
8. Ghosh E, Dwivedi H, Baidya M, et al. Conformational sensors and domain swapping reveal structural and functional differences between β -arrestin isoforms. *Cell Rep.* 2019;28:3287-3299.
 9. Thomsen ARB, Plouffe B, Cahill TJ 3rd, et al. GPCR-G protein- β -arrestin super-complex mediates sustained G protein signaling. *Cell.* 2016;166:907-919.
 10. Irannejad R, Tomshine JC, Tomshine JR, et al. Conformational biosensors reveal GPCR signalling from endosomes. *Nature.* 2013;495:534-538.
 11. Tsvetanova NG, von Zastrow M. Spatial encoding of cyclic AMP signaling specificity by GPCR endocytosis. *Nat Chem Biol.* 2014;10:1061-1065.
 12. Kallal L, Gagnon AW, Penn RB, Benovic JL. Visualization of agonist-induced sequestration and down-regulation of a green fluorescent protein-tagged β 2-adrenergic receptor. *J Biol Chem.* 1998;273:322-328.
 13. Moore RH, Sadovnikoff N, Hoffenberg S, et al. Ligand-stimulated beta 2-adrenergic receptor internalization via the constitutive endocytic pathway into Rab5-containing endosomes. *J Cell Sci.* 1995;108:2983-2991.
 14. Scarselli M, Donaldson JG. Constitutive internalization of G protein-coupled receptors and G proteins via clathrin-independent endocytosis. *J Biol Chem.* 2009;284:3577-3585.
 15. von Zastrow M, Kobilka BK. Ligand-regulated internalization and recycling of human Beta2-adrenergic receptors between the plasma membrane and endosomes containing transferrin receptors. *J Biol Chem.* 1992;267:3530-3538.
 16. Kilpatrick LE, Alcobia DC, White CW, et al. Complex formation between VEGFR2 and the β 2-adrenoceptor. *Cell Chem Biol.* 2019;26:830-841.
 17. Dishy V, Sofowora GG, Xie HG, et al. The effect of common polymorphisms of the β 2-adrenergic receptor on agonist-mediated vascular desensitization. *N Engl J Med.* 2001;345:1030-1035.
 18. Green SA, Turki J, Bejarano P, Hall IP, Liggett SB. Influence of beta 2-adrenergic receptor genotypes on signal transduction in human airway smooth muscle cells. *Am J Respir Cell Mol Biol.* 1995;13:25-33.
 19. Green SA, Turki J, Innis M, Liggett SB. Amino-terminal polymorphisms of the human beta.2-adrenergic receptor impart distinct agonist-promoted regulatory properties. *Biochemistry.* 1994;33:9414-9419.
 20. Koryakina Y, Jones SM, Cornett LE, et al. Effects of the β -agonist, isoprenaline, on the down-regulation, functional responsiveness and trafficking of β 2-Adrenergic receptors with N-terminal polymorphisms. *Cell Biol Int.* 2012;36(12):1171-1183.
 21. Kobilka BK, Dixon RA, Frielle T, et al. cDNA for the human beta 2-adrenergic receptor: a protein with multiple membrane-spanning domains and encoded by a gene whose chromosomal location is shared with that of the receptor for platelet-derived growth factor. *Proc Natl Acad Sci U S A.* 1987;84(1):46-50.
 22. Reihnsaus E, Innis M, MacIntyre N, Liggett SB. Mutations in the gene encoding for the beta 2-adrenergic receptor in normal and asthmatic subjects. *Am J Respir Cell Mol Biol.* 1993;8(3):334-339.
 23. Green SA, Cole G, Jacinto M, Innis M, Liggett SB. A polymorphism of the human beta 2-adrenergic receptor within the fourth transmembrane domain alters ligand binding and functional properties of the receptor. *J Biol Chem.* 1993;268(31):23116-23121.
 24. Hawkins GA, Tantisira K, Meyers DA, et al. Sequence, haplotype, and association analysis of ADR β 2 in a multi-ethnic asthma case-control study. *Am J Respir Crit Care Med.* 2006;174:1101-1109.
 25. Dewar JC, Wheatley AP, Venn A, Morrison JFJ, Britton J, Hall IP. Beta2-adrenoceptor polymorphisms are in linkage disequilibrium, but are not associated with asthma in an adult population. *Clin Exp Allergy.* 1998;28:442-448.
 26. Stallaert W, Dorn JF, van der Westhuizen E, Audet M, Bouvier M. Impedance responses reveal β 2-adrenergic receptor signaling pluridimensionality and allow classification of ligands with distinct signaling profiles. *PLoS ONE.* 2012;7(1):e29420.
 27. Lamichhane R, Liu JJ, Pljevaljcic G, et al. Single-molecule view of basal activity and activation mechanisms of the G protein-coupled receptor β 2 AR. *Proc Natl Acad Sci U S A.* 2015;112:14254-14259.
 28. Gregorio GG, Masureel M, Hilger D, et al. Single-molecule analysis of ligand efficacy in β 2AR-G-protein activation. *Nature.* 2017;547:68-73.
 29. Sun Y, Li N, Zhang M, et al. Single-molecule imaging reveals the stoichiometry change of β 2-adrenergic receptors by a pharmacological biased ligand. *Chem Commun.* 2016;52:7086-7089.
 30. Calebiro D, Grimes J. G protein-coupled receptor pharmacology at the single-molecule level. *Annu Rev Pharmacol Toxicol.* 2020;60:73-87.
 31. Grime RL, Goulding J, Uddin R, et al. Single molecule binding of a ligand to a G-protein-coupled receptor in real time using fluorescence correlation spectroscopy, rendered possible by nano-encapsulation in styrene maleic acid lipid particles. *Nanoscale.* 2020;12(21):11518-11525.
 32. Spence JR, Mayhew CN, Rankin SA, et al. Directed differentiation of human pluripotent stem cells into intestinal tissue in vitro. *Nature.* 2011;470:105-109.
 33. Huang SXL, Islam MN, O'Neill J, et al. Efficient generation of lung and airway epithelial cells from human pluripotent stem cells. *Nat Biotechnol.* 2014;32:84-91.
 34. Denning C, Allegrucci C, Priddle H, et al. Common culture conditions for maintenance and cardiomyocyte differentiation of the human embryonic stem cell lines, BG01 and HUES-7. *Int J Dev Biol.* 2006;50:27-37.
 35. White CW, Caspar B, Vanyai HK, Pflieger KDG, Hill SJ. CRISPR-mediated protein tagging with nanoluciferase to investigate native chemokine receptor function and conformational changes. *Cell Chem Biol.* 2020;27:499-510.
 36. Calebiro D, Rieken F, Wagner J, et al. Single-molecule analysis of fluorescently labeled G Protein-coupled receptors reveals complexes with distinct dynamics and organization. *Proc Natl Acad Sci U S A.* 2013;110:743-748.
 37. Regard JB, Sato IT, Coughlin SR. Anatomical profiling of G protein-coupled receptor expression. *Cell.* 2008;135:561-571.
 38. Rose RH, Briddon SJ, Hill SJ. A novel fluorescent histamine H1 receptor antagonist demonstrates the advantage of using fluorescence correlation spectroscopy to study the binding of lipophilic ligands. *Br J Pharmacol.* 2012;165:1789-1800.
 39. Briddon SJ, Middleton RJ, Cordeaux Y, et al. Quantitative analysis of the formation and diffusion of A1-adenosine receptor-antagonist complexes in single living cells. *Proc Natl Acad Sci U S A.* 2004;101:4673-4678.
 40. Briddon SJ, Kilpatrick LE, Hill SJ. Studying GPCR pharmacology in membrane microdomains: fluorescence correlation spectroscopy comes of age. *Trends Pharmacol Sci.* 2018;39:158-174.

41. Chiantia S, Ries J, Schwille P. Fluorescence correlation spectroscopy in membrane structure elucidation. *Biochim Biophys Acta Biomembr.* 2009;1788:225-233.
42. Corriden R, Kilpatrick LE, Kellam B, Briddon SJ, Hill SJ. Kinetic analysis of antagonist-occupied adenosine-A3 receptors within membrane microdomains of individual cells provides evidence of receptor dimerization and allostereism. *FASEB J.* 2014;28:4211-4222.
43. Gondin AB, Halls ML, Canals M, Briddon SJ. GRK mediates μ -opioid receptor plasma membrane reorganization. *Front Mol Neurosci.* 2019;12:104.
44. Herrick-Davis K, Grinde E, Cowan A, Mazurkiewicz JE. Fluorescence correlation spectroscopy analysis of serotonin, adrenergic, muscarinic, and dopamine receptor dimerization: the oligomer number puzzle. *Mol Pharmacol.* 2013;84:630-642.
45. Gherbi K, May LT, Baker JG, Briddon SJ, Hill SJ. Negative cooperativity across β 1-adrenoceptor homodimers provides insights into the nature of the secondary low-affinity CGP 12177 β 1-adrenoceptor binding conformation. *FASEB J.* 2015;29:2859-2871.
46. Dixon JR, Selvaraj S, Yue F, et al. Topological domains in mammalian genomes identified by analysis of chromatin interactions. *Nature.* 2012;485:376-380.
47. Kondrashov AV, Kiefmann M, Ebnet K, Khanam T, Muddashetty RS, Brosius J. Inhibitory effect of naked neural BC1 RNA or BC200 RNA on eukaryotic in vitro translation systems is reversed by poly(A)-binding protein (PABP). *J Mol Biol.* 2005;353:88-103.
48. Dick E, Matsa E, Bispham J, et al. Two new protocols to Enhance the production and isolation of human induced pluripotent stem cell lines. *Stem Cell Res.* 2011;6:158-167.
49. Matsa E, Rajamohan D, Dick E, et al. Drug evaluation in cardiomyocytes derived from human induced pluripotent stem cells carrying a long QT syndrome type 2 mutation. *Eur Heart J.* 2011;32:952-962.
50. White CW, Vanyai HK, See HB, Johnstone EKM, Pflieger KDG. Using NanoBRET and CRISPR/Cas9 to monitor proximity to a genome-edited protein in real-time. *Sci Rep.* 2017;7:3187.
51. Cowan CA, Klimanskaya I, McMahon J, et al. Derivation of embryonic stem-cell lines from human blastocysts. *N Engl J Med.* 2004;350:1353-1356.
52. Kondrashov A, Duc Hoang M, Smith JGW, et al. Simplified footprint-free Cas9/CRISPR editing of cardiac-associated genes in human pluripotent stem cells. *Stem Cells and Dev.* 2018;27:391-404.
53. Keppler A, Gendreizig S, Gronemeyer T, Pick H, Vogel H, Johnsson KA. General method for the covalent labeling of fusion proteins with small molecules in vivo. *Nat Biotechnol.* 2003;21:86-89.
54. Ayling LJ, Briddon SJ, Halls ML, et al. Adenylyl cyclase AC8 directly controls its microenvironment by recruiting the actin cytoskeleton in a cholesterol-rich milieu. *J Cell Sci.* 2012;125:869-886.
55. Huang B, Perroud TD, Zare RN. Photon counting histogram: one-photon excitation. *ChemPhysChem.* 2004;5:1523-1531.
56. Nesbeth D, Williams SL, Chan L, et al. Metabolic biotinylation of lentiviral pseudotypes for scalable paramagnetic microparticle-dependent manipulation. *Mol Ther.* 2006;13:814-822.
57. Bruck H, Leineweber K, Büscher R, et al. The Gln27Glu Beta2-Adrenoceptor polymorphism slows the onset of desensitization of cardiac functional responses in vivo. *Pharmacogenetics.* 2003;13:59-66.
58. Bruck H, Leineweber K, Park J, et al. Human β -Adrenergic receptor gene haplotypes and venodilation in vivo. *Clin Pharmacol Ther.* 2005;78:232-238.
59. Rosethorne EM, Turner RJ, Fairhurst RA, Charlton SJ. Efficacy is a contributing factor to the clinical onset of bronchodilation of inhaled beta(2)-adrenoceptor agonists. *Naunyn Schmiedebergs Arch Pharmacol.* 2010;382:255-263.
60. İşbilir A, Möller J, Arimont M, et al. Advanced fluorescence microscopy reveals disruption of dynamic CXCR4 dimerization by subpocket-specific inverse agonists. *Proc Natl Acad Sci U S A.* 2020;117:29144-29154.
61. Scarselli M, Annibale P, Radenovic A. Cell type-specific β 2-adrenergic receptor clusters identified using photoactivated localization microscopy are not lipid raft related, but depend on actin cytoskeleton integrity. *J Biol Chem.* 2012;287:16768-16780.
62. Wingler LM, Lefkowitz RJ. Conformational basis of G protein-coupled receptor signaling versatility. *Trends Cell Biol.* 2020;30(9):736-747.
63. Murphy L, Rennard S, Donohue J, et al. Turning a molecule into a medicine: the development of indacaterol as a novel once-daily bronchodilator treatment for patients with COPD. *Drugs.* 2014;74:1635-1657.
64. Jacobson GA, Raidal S, Hostrup M, et al. Long-acting β 2-agonists in asthma: enantioselective safety studies are needed. *Drug Saf.* 2018;41:441-449.

SUPPORTING INFORMATION

Additional Supporting Information may be found online in the Supporting Information section.

How to cite this article: Goulding J, Kondrashov A, Mistry SJ, et al. The use of fluorescence correlation spectroscopy to monitor cell surface β 2-adrenoceptors at low expression levels in human embryonic stem cell-derived cardiomyocytes and fibroblasts. *The FASEB Journal.* 2021;35:e21398. <https://doi.org/10.1096/fj.202002268R>